



Antecedent geological control on transgressive delta and shoreline preservation: Examples from the SE African shelf

Engelbrecht, L., Green, A. N., Cooper, A., & Mackay, F. (2022). Antecedent geological control on transgressive delta and shoreline preservation: Examples from the SE African shelf. *Marine Geology*, 454, 1-16. Article 106934. Advance online publication. <https://doi.org/10.1016/j.margeo.2022.106934>

[Link to publication record in Ulster University Research Portal](#)

Published in:
Marine Geology

Publication Status:
Published (in print/issue): 31/12/2022

DOI:
[10.1016/j.margeo.2022.106934](https://doi.org/10.1016/j.margeo.2022.106934)

Document Version
Author Accepted version

General rights
Copyright for the publications made accessible via Ulster University's Research Portal is retained by the author(s) and / or other copyright owners and it is a condition of accessing these publications that users recognise and abide by the legal requirements associated with these rights.

Take down policy
The Research Portal is Ulster University's institutional repository that provides access to Ulster's research outputs. Every effort has been made to ensure that content in the Research Portal does not infringe any person's rights, or applicable UK laws. If you discover content in the Research Portal that you believe breaches copyright or violates any law, please contact pure-support@ulster.ac.uk.

Antecedent geological control on transgressive delta and shoreline preservation: examples from the SE African shelf.

L. D. Engelbrecht¹, A. N. Green², J. A. G. Cooper³, C. F. Mackay⁴.

¹Geological Sciences, University of KwaZulu-Natal, Westville, Private Bag X54001, South Africa

²School of Geography and Environmental Sciences, Ulster University, Coleraine BT52 ISA, Northern Ireland, United Kingdom

³Oceanographic Research Institute, PO Box 10712 Marine Parade 4056, Durban, South Africa

⁴School of Life Sciences, University of KwaZulu-Natal, Durban, Private Bag X54001, South Africa

Abstract

Using a suite of ultra-high resolution geophysical tools, remote operated vehicle dives, and isolated grab samples, we demonstrate at a regional shelf scale, the influence of antecedent geology (basement topography, shelf gradient and submerged shoreline features) on the evolving transgressive shelf stratigraphy of a subaqueous delta. The unconsolidated uppermost delta occurs as isolated remnants scattered across the low-gradient shelf. Seismic data reveal across-shelf heterogeneity in bedrock elevation, with prominent bedrock highs and depressions and several well-preserved aeolianite palaeo-shoreline complexes at water depths of -100, -60 and -40 m. Analysis of bathymetric and seismic data demonstrates that these pre-existing shoreline complexes exert an overarching control on the distribution patterns of i) deltaic sediments, where they abut the landward flank of the shoreline form, acting as a barrier to seaward dispersal, and ii) shoreface sediments which remain sequestered on the mid-shelf on the seaward flank of the shoreline complex, hampering the landward translation of the

shoreface in step with rising sea levels. Moreover, sediment distribution/accumulation is further constrained where elevated portions of the basement topography provide little to no accommodation, and act as zones of sediment bypass, and adjacent basement depressions accommodate sediment to seaward. The gentle antecedent slope, coupled with the gentle shoreline trajectory mediated transgressive erosion directly to landward. This is reinforced where local inflections in the wave ravinement profile form due to the presence of palaeo-shoreline complexes, aiding in the ultimate preservation of these submerged delta facets in the palaeo-shoreline lee. This study shows that low antecedent gradients, and palaeo-shoreline features, lead to development of transgressive coastal profiles that are predisposed to delta overstepping. The pre-existing basement topography and palaeo-shorelines constrain the positioning and morphology of the delta. We suggest that antecedent conditioning has partitioned accommodation for delta accumulation and moderated wave ravinement associated with transgression since the Last Glacial Maximum (LGM). The geological framework has acted as a recurring primary control to the geomorphic evolution of the submarine delta and shelf.

Keywords

Submerged deltas; antecedent geology; palaeo-shorelines; Thukela shelf

1. Introduction

In the context of rapidly rising sea-levels, and the threat they pose to modern urban coastlines, there has been an urgency to define models that pinpoint the major forcing factors that govern the evolution of littoral systems and the resultant transgressive stratigraphy. Much attention has focussed on deltas (e.g., Syvitski et al., 2009; Vörösmarty et al., 2009; Milliman and Farnsworth, 2011; Besset et al., 2019; Engelbrecht et al., 2020; Dyer et al., 2021) and barrier

shoreline evolution (e.g., Locker et al., 1996; Cooper, 1991; Gardner et al., 2005, 2007; Storms et al., 2008; Mellet et al., 2012; Green et al., 2013a, 2014).

Construction and preservation of these coastal features is generally interpreted in the context of the complex interplay between sea-level variability and sediment supply. Continental shelves, however, exhibit significant additional local variability expressed as heterogeneity in framework/antecedent geological control that is often overlooked in models of transgressive stratigraphy. These act locally to influence sedimentation in response to sea-level changes and are an important control on the morphological evolution of coastal environments (Holland & Elmore, 2008, Cooper et al., 2018a).

While antecedent control is acknowledged by some authors (Bortolin et al., 2018; Kirkpatrick and Green, 2018; Kirkpatrick et al., 2019; Mallinson et al., 2010; Engelbrecht et al., 2020; Dyer et al., 2021; Gal et al., 2021), there are very few explicit demonstrations of its role. Exceptions to this include studies from the continental shelf and coast of Virginia (Shawler et al., 2020), North Carolina (Riggs et al., 1995) and the Outer Hebrides of Scotland (Cooper et al., 2012).

In this paper, using data from the entire shelf width and along a 150 km length of coastline, we investigate the influence of antecedent geology (basement topography, shelf gradient and submerged shoreline features) on the evolving stratigraphy of the deltaic Thukela shelf throughout the postglacial marine transgression.

2. Regional Setting

2.1. Physiography

The KwaZulu-Natal shelf (Fig. 1) on average is steep (0.24°) and narrow (18 km) (Green et al., 2013b) compared to global averages for shelf gradient (0.12°) and width (73 km) (Shepard, 1963). However, the Thukela shelf between Durban and Richards Bay comprises a considerably broadened and flatter feature (~ 45 km and 0.13° respectively, Martin and Flemming, 1986), close to the global average. This is attributed to a structural offset, ascribed to a change in tectonic origin of the margin from a sheared to a short-rifted section (Martin and Flemming 1988). The shelf break is situated at ~ 100 m water depth (Green et al., 2013b), and the shelf edge is dominated by the poleward-flowing Agulhas Current.

2.2. Geology

The shelf forms part of the Durban Basin, a complex Mesozoic rifted feature which originated along the east African continental plate prior to the breakup of Gondwana (Dingle and Scrutton, 1974; Dingle et al., 1983; Broad et al., 2006). During early Cretaceous a deep-water fan complex (Thukela Cone) began prograding into the Natal Valley area (Goodlad, 1986). Thereafter, late Campanian to late Maastrichtian aged marine claystones were deposited as a >900 m thick succession. The study area is underlain by Pliocene-aged rocks, forming the base upon which a thin veneer of Pleistocene (offshore palaeo-dune cordons, preserved as coast-parallel, submerged reef systems) and Holocene (restricted to modern day progradational highstand sediment prism) sediments were deposited (Martin and Flemming, 1988; Ramsay, 1994; Bosman et al., 2007; Green and Garlick, 2011).

2.3. Sediment supply

The structural offset and broadened continental shelf of the Thukela shelf, causes a change in shelf orientation relative to the southward flowing Agulhas Current, and results in the

generation of a semi-permanent equatorward counter-current gyre inshore (Flemming, 1981, Schumann, 1988; Grundlingh, 1992). This gyre, centred on the Thukela shelf, receives its primary source of direct terrigenous sediment input by means of fluvial discharge (Flemming, 1981), in particular from the Thukela River, the largest river on the KwaZulu-Natal coastline.

Other sources of sediment input to the shelf include i) entrainment of sediment from the northward directed longshore current (McCormick et al., 1992; Green and Mackay, 2016) whereby SE swells with significant average wave heights between 1.8 m and 1.5 m, disperse sediment northwards in the littoral regions of the wave-dominated shelf (Green and Mackay, 2016), and ii) biogenic production (Flemming and Hay, 1988). A spring tidal range of 1.8 m (Moes and Rossouw, 2008), places the coastline in the microtidal range.

2.4. Sea levels

Glacio-eustatic sea levels have risen from the Last Glacial Maximum (LGM) ~18 ka BP, when the shelf was subaerially exposed with a shoreline at ~ 125 m below present levels (Cooper et al., 2018b), up to a highstand level of +3.5 m around 5.5 ka BP. Superimposed on the overall rise in sea level were alternating periods of slower and accelerated rates of sea-level rise (Cooper et al., 2018b); each of which corresponded to the development and later overstepping of coastal landforms respectively (Pretorius et al., 2016). The preservation of these landforms at -100 m and -60 m is ascribed to subsequent rapid inundation of the landform by rapid jumps in base level associated with Meltwater Pulses (MWP) 1A and 1B (Fig. 2) respectively (Salzmann et al., 2013; Pretorius et al., 2016, 2019). MWP-1A, from a base level of ~ 100 m lower than present, was initiated at the onset of the Bølling–Allerod Interstadial ~14.65 ka BP, characterised by a pronounced acceleration (~40 mm year⁻¹) (Deschamps et al., 2012) of base level rise (Stanford et al., 2011). Although there has been much debate over the attribution of

a period of accelerated sea level rise following the Younger Dryas from 12.7 ka BP to a second post-glacial meltwater pulse, there is substantial evidence that this period was defined by episodes of fleeting rates of sea level rise (Camoin et al., 2004, Lambeck et al., 2014). MWP-1B has been inferred from various localities globally, with up to 40 mm year⁻¹ leaps in base level assumed from records in Barbados (Liu and Milliman, 2004; Abdul et al., 2016).

3. Methods

Approximately 1500 line km of ultra-high seismic reflection and multibeam bathymetric data were collected between the 31st January and 6th February 2018 aboard the RV Dr. Fridtjof Nansen (Fig. 1). These spanned the southern portions of the Thukela shelf, up to Cape St Lucia and covered an area of 3400 km² (Fig. 1). Seismic reflection data were collected using a Kongsberg PS40 Topas parametric sub bottom profiler in Chirp mode. The data were processed using the Kongsberg SBP utility where they were match filtered and the secondary frequency between 1-10 kHz output. These data resolve to ~ 20 cm in the vertical domain. The data were further processed and interpreted in the Hypack SBP utility where they were bottom tracked and swell filtered. All time to depth conversions were applied using values of 1500 m.s⁻¹ in water and 1600 m.s⁻¹ in sediment.

Multibeam data were collected using a Kongsberg EM710 very high resolution echosounder. Sound velocity changes in the water column were examined using regular casts of a Seabird 911 Conductivity-Temperature-Depth (CTD) sensor. All data were processed using Beamworx software, where spurious soundings were removed and the data reduced to MSL using South African Navy tide charts (SAN, 2018). The final data were gridded at a resolution of 2 x 2 m.

A Seaeye falcon Remote Operated Vehicle (ROV) was employed to groundtruth the multibeam data, in tandem with a drop camera and legacy grab samples described in Green and MacKay (2016). A suite of legacy vibracore data, collected as part of a previous heavy minerals prospecting campaign in the early 2000's, were also integrated into the study to assist with seismic stratigraphic interpretations. The cores were logged before bulk sampling and unfortunately no material for further sampling for age chronology was available.

4. Results

4.1 Seismic Stratigraphy

Eight seismic units were resolved across the Thukela continental shelf, identified by the seismic impedance of internal reflections, internal reflection configuration, reflection termination patterns and bounding acoustic reflectors.

4.1.1 Unit 1

Unit 1, the oldest and lowermost unit (Figs. 3, 6-9) comprises the acoustic basement of this study. It is characterised by continuous, inclined-parallel high amplitude reflectors that dip gently seaward. The lower surface of the basement unit is obscured by the multiple in shallower water and lies below the penetration capabilities of the seismic system in deeper water.

The uppermost reflectors of Unit 1 are truncated by a high amplitude reflector (Figs. 3 and 8), SB1, which marks the clear discordant relationship between Unit 1 and the overlying stratigraphy.

These SB1 incisions have been carved into the uppermost portions of the underlying Unit 1, predominantly the mid-shelf region. The incisions vary in width (tens of metres to kilometres wide) and depth (average between 15 m and 25 m). In the northern part of the study area, SB1 crops out as an elevated high of Unit 1 and forms a gently easterly-dipping irregular pavement intersected by two prominent low-points up to 10 m in relief and ~ 1.9 km-wide (Figs. 4, 6 and 7).

4.1.2 Unit 2

Unit 2, a series of pinnacles, ridges and fills that occur directly overlying SB1, are observed in depth defined clusters across the shelf, from 30 m to 100 m depths. Based on its seismic expression, Unit 2 can be subdivided into two subunits (Units 2.1, and 2.2).

Unit 2.1 comprises a series of acoustically opaque blocks and pinnacles that limit signal penetration and visualisation of the reflectors beneath. Between depths of -60 m to -100 m, Unit 2.1 occurs as a discontinuous series of high relief, 20 - 25 m high pinnacles. These ridge-like features crop out on the contemporary sea floor as sharp positive relief anomalies surrounded by an otherwise smooth sea floor (Figs. 3, 6 and 7). The down-dip extent of Unit 2.1 is discontinuous and sporadic, yet its basal contact with the basement occurs consistently at several prominent depths. The first complex of high relief pinnacles occurs with the pinnacle bases at ~100 m at or near the shelf break, with a second cluster of pinnacles to landward at ~60 m basal depth. A third cluster of pinnacles and ridges occur between 30 m and 40 m basal depths (Figs. 6 and 7).

Remotely Operated Vehicle (ROV) footage shows overhangs developed in the high angle planar foresets (Fig. 5a) of Unit 2.1. Grab samples obtained immediately adjacent to the outcrop of Unit 2.1 reveal the adjoining sediment to comprise beachrock fragments with shell hash and occasional siltstone clasts. The prices of Unit 2.1 retrieved by grabs comprise a medium grained, blocky calcite-cemented sandstone, with shell and fragments, and peloids.

Unit 2.2 rests within the saddles created between the high relief pinnacles of Unit 2.1 (Figs. 3, 6 and 7) where its reflections onlap the walls of the high relief structures. These reflections comprise moderate to high amplitude, horizontal to sub-horizontal reflections. Unit 2.2 also onlaps the seaward and landward margins of the Unit 2.1 pinnacles.

4.1.3 Unit 3

Unit 3 occurs exclusively within the incisions carved into the underlying Unit 1 by SB1 (Fig. 3), comprising a variety of low to high amplitude reflectors with chaotic internal reflector configurations. These reflectors onlap the steep valley walls of SB1. Unit 3 fills incisions in SB1 of 10 - 25 m in relief and from tens of metres to up to 1 km in width. Unit 3 occurs sporadically, with across and along-shelf exposure limited.

4.1.4 Unit 4

Unconformably draping the highly irregular truncated upper portions of Unit 1 in the proximal to mid-shelf regions, lies the uniformly 3-5 m thick, laterally extensive sediment body of Unit 4. This is characterised by flat-lying to slightly sigmoidal, low to moderate amplitude progradational reflections comprising an overall backstepping pattern. Unit 4 mostly abuts the

landward side of the shallower exposures of the steep pinnacles of Unit 2.1 (Figs. 3 and 9) however it also occurs intermittently to seaward of them (Fig. 3), where the reflectors downlap the underlying SB1, or onlap it where there is sub or outcropping basement geology. Unit 4 is completely restricted to the low gradient, flat-lying portions of the inner-mid shelf and is absent from the steeper areas at or near the shelf break.

4.1.5 Unit 5

Unit 5 occurs in distinct distal and proximal depocenters with a variety of internal reflections, which range from acoustically transparent to high amplitude in character. Distally, Unit 5 comprises low to moderate amplitude, discontinuous mounded to progradational reflections (Figs. 3, 7 and 8). Maximum thicknesses of Unit 5 (up to 15 m) occur where the unit onlaps the landward side of the pinnacles of Unit 2.1 (Figs. 3 and 7). Unit 5 may also downlap onto the underlying basement Unit 1.

Proximally, Unit 5 comprises a variety of reflector configurations, ranging from low amplitude, parallel, flat-lying reflector sets at its base where they onlap and downlap both the underlying Unit 4 and SB1 (upper bounding surface of Unit 1), to mounded to sigmoid progradational reflectors in its uppermost and most seaward portions. Unit 5 onlaps Unit 2.1 in the mid shelf (Figs. 3 and 9), where the steep pinnacles limit its down-dip continuity. The maximum thickness of 10 - 12 m correlates to local depressions/ low-lying regions within the underlying basement unit (Figs. 7 and 8), notably where aggradational to progradational lobes of sediment accumulate. The topset break of the upper sigmoid reflectors occurs at a depth of ~35 – 40 m. Where the basement unit is elevated, Unit 5 is very thinly developed or absent completely.

4.1.6 Unit 6

Like Unit 5, Unit 6 occurs in distinct depocenters, closely associated with the underlying Unit 5. The distal portions of Unit 6 are characterised by continuous, low to moderate amplitude flat-lying reflectors, the uppermost portions of which are exposed as a smooth veneer along the contemporary sea floor. However, where Unit 6 is located between the pinnacles of Unit 2.1 against which it abuts, the uppermost portions occur as moderate amplitude, prograding reflectors with an undulatory upper surface, often resulting in a positive relief sea floor expression. The seaward extension of Unit 6 in the deepest and most distal regions of the shelf, is commonly impeded and obstructed by the positive relief of the ridge-like outcrops of Unit 2.1, interrupting its down-dip continuity across the outer shelf (Figs. 3 and 7).

The proximal depocenters of Unit 6 occur as a seaward prograding wedge near to and overlying Unit 5 at water depths ranging from 30 – 40 m. Here, they are characterised by the occasional mounded to more flat-lying prograding low to moderate amplitude reflectors. The proximal depocenters reach a maximum thickness of 8 m. Unit 6 downlaps the underlying Unit 5, or where it progrades past the seaward down dip extremities of Unit 5, downlaps and onlaps Unit 1 and SB1. Unit 6 also onlaps Unit 2.1 proximally, where Unit 2.1 limits the down dip continuation of Unit 6 to seaward. The topset break of the proximal depocenter is observed at ~30 – 35 m. Where Units 5 and 6 are at their thickest (the topset break point), a matching positive relief in the sea floor is observed (Figs. 3, 7, 8 and 9).

The uppermost portions of Units 4, 5, and 6 are truncated by a high amplitude reflector (Fig. 8), wRS. This surface forms a uniformly seaward dipping erosional surface, except where it

steepens in conjunction with positive relief displayed by the thicker accumulations of Units 5 and 6.

4.1.7 Unit 7

Unit 7 occurs as an isolated unit on the seaward edge of Unit 2.1. It is characterised by an up to 8-m-thick wedge of moderate to high amplitude prograding reflectors which downlap the uppermost reflectors of the underlying Unit 6. The upper undulatory portions of Unit 7 form part of the seafloor.

4.1.8 Unit 8

Unit 8 occurs primarily in the proximal to mid-shelf regions, draping local depressions/low-lying portions of shelf between units that impart a positive relief to the sea floor (Figs. 8 and 9), such as Units 2.1, 5 and 6. Unit 8 is characterised by flat-lying, continuous, aggradational very low amplitude reflections with occasional transparent patches. The unit varies from 3 to 5 m-thick, and onlaps wRS to form the contemporary sea floor of the inner shelf.

4.2 Lithostratigraphy

Core 24

Core 24 (Figs. 6 and 10) was retrieved from a water depth of -30 m. The 283 cm long core comprises a fining upwards succession of Units 5, 6 and 7. From -283 cm to -110 cm depth, are featureless, light brown, slightly muddy fine sands of Unit 5. Capping this is a 10 cm-thick, light brown, poorly sorted, coarse-grained shelly sand that marks the upper limit of Unit 5.

From -100 cm to -50 cm, a moderately sorted, slightly muddy fine to medium grey sand defines the intersection with Unit 6. 50 cm-thick grey, very soft mud, caps the overall fining upward succession and represents Unit 8.

Core 22

Core 22 is 220 cm long and was retrieved from a water depth of -34 m (Figs. 6 and 10). The core penetrates an accumulation of sediment landward of a prominent bedrock high that marks a change from a zone of sediment accumulation of Units 5 and 6, to a zone of lower accumulation where there is sub- and outcropping of Unit 1 basement strata. From 220 cm to a depth of 198 cm, the core intersects brown, medium to coarse, poorly sorted sands, with shell fragments and heavy minerals of Unit 5 (Fig. 10). Mantling this is an ~10 cm-thick dark grey soft mud, which abruptly transitions into a medium sand with visible heavy minerals, and gently grades into a well sorted, muddy to fine sand where it intercepts the sea floor, constituting Unit 6.

Core 21

Core 21 (Figs. 6 and 10) was retrieved from a water depth of -52 m and penetrates Unit 6 and terminates on the upper surface of Unit 5. The 59 cm-long core consists primarily of fine to medium sand, with indurated semi-rounded clasts 3-4 cm in diameter from its base up to a depth of ~10 cm. The wRS crops out at the seabed above unit 6. The uppermost 10 cm of the core consists of a bioclastic conglomerate comprising bivalves, gastropods and bryozoa fragments, within a dark brown sandy matrix.

Core 23

Core 23 penetrates Units 5, 6 and 7, where the thickest across-shelf accumulation of sediment occurs within a distinct bedrock depression (Figs. 8 and 10). Shell debris is distributed throughout the succession, except near the top where the mud-dominated sections occur. Unit 5 (base to 105 cm) comprises a fine to medium sand, capped by a 5-cm-thick shell hash of broken bivalves representing wRS (Fig. 10). This is overlain by a fining upward succession of Units 6 and 8 composed of medium sand and a soft sandy respectively.

4.3 Sea floor morphology and shallow subsurface geomorphology

High-resolution multibeam bathymetric mapping (Fig. 11) reveals an area of sea floor characterized by shore-parallel (NE-SW orientated), high relief ridges (averaging ~5 m and up to >15 m high and up to 100 m wide). These form continuous along-strike features for > 10 km. These ridges of Unit 2.1 are concentrated between the shelf break and depths of 60 m below sea level, the crests of the two most prominent of which occur at depths between 55 m – 75 m (Fig. 11c) and 90 m – 95 m (Fig. 11e). The shallower ridge varies in its along-shelf expression. To the north, it is a single, narrow (80 m-wide), continuous and straight-crested ridge (Fig. 11b) contrasting to the south where it occurs as a series of discontinuous, parabolic-shaped ridges of Unit 2.1 with an area of raised sea floor spanning up to 500 m wide (Fig. 11a). Similarly, the deeper ridge also has a contrasting morphology from north to south. In the north it comprises a single, narrow, continuous and straight-crested ridge (Fig. 11b) while in the south, the ridge forms is abutted by a series of recurved ridges of Unit 2.1 that enclose a shallow (< 5 m) depression (Fig. 11d). Another series of depressions occur south of this, into which cusped wedges of unit 2.1 protrude and create isolated, semi-circular seafloor depressions (Fig. 11a).

Flat seafloor fronts the seaward edges of the ~ 95 m and ~ 60 m ridges, where wRS is exposed in outcrop forming a platform at -95 and -65 m (Figs. 11e, f; 12 c, d). Between these two prominent ridges is an area of rugged sea floor with less prominent ridges composed of Unit 1.

The distribution and thickness of Unit 2.1, in both outcrop and subcrop is shown in figures 12a and b. The distribution is very similar to that mapped from the multibeam bathymetry, however the shore-parallel, linear ridges are clearer. The thickest accumulation of Unit 2 corresponds to the -60 m ridges and the -100 m ridges. Some deeper exposures of Unit 2 are present in the south and occur in the arcuate scarps of several small landslides at ~ -120 m (Fig. 12a).

In the south, there are virtually no unconsolidated sediments overlying Unit 2 and wRS (Fig. 12c). Isolated patches of sediment mantle depressions that occur between the parabolic-shaped ridges of the -60 m ridge, with other isolated pockets occurring sporadically. These reach a maximum thickness of 1 m. To the north and directly seawards of the -60 m ridge is a 10 m-thick zone of sediment that overlies Unit 2 and wRS. This is a departure from the typically sediment-scarce outer shelf regions of the SE African shelf (Flemming, 1978; 1988). This unconsolidated sediment is organised into large to very large subaqueous dunes with their slip faces oriented to the south.

5. Discussion

5.1. Seismic stratigraphic interpretation

5.1.1. Acoustic basement

Unit 1, the oldest seismic unit, constitutes the acoustic basement for this study. Predicated on its overall stratigraphic position, identified as the lowermost resolvable seismic unit in the study area, and its distinctive seaward progradational reflectors (Figs. 3, 6-9), this unit conforms to descriptions of late Pliocene age siltstones that subcrop the mid to outer shelf of the area (Hicks and Green, 2016). These siltstones form a prominent high point in the area to the north of the modern aMatigulu River at a depth of 32 m.

Unit 1 is truncated by SB1 (Fig. 8). This channelled surface is commonly recognised across the SE African shelf (Green et al., 2013b), and represents the subaerial unconformity associated with the LGM (Pretorius et al., 2016). In a significant departure from the densely arranged drainage patterns preserved on the shelf to the south (Green and Garlick, 2011; Green et al., 2013b; Pretorius et al., 2019), the study area is largely devoid of a distinct drainage configuration, particularly from the mid-shelf to the shelf break where only a few underfilled channels are evident. Engelbrecht et al. (2020) also identified limited evidence of fluvial channels in the shallow nearshore regions of the Thukela shelf, with a reduction in incised valley density basinwards. The incised valley fill component is represented by Unit 3.

5.1.2. Palaeo-shorelines and aeolianite rubble

The well-defined, narrow and tall coast-parallel ridges of Unit 2.1 are similar to the aeolianite and beachrock shorelines described by others for the SE African shelf (De Lecea et al., 2017; Dyer et al., 2021; Green et al., 2014; Salzmann et al., 2013; Pretorius et al., 2016; Green et al., 2013b, 2014, 2020). ROV and drop camera footage confirm that Unit 2.1 comprises sandy calcareous blocks with high-angle foresets typical of coastal aeolianites (Cooper and Flores, 1991; Cooper and Green, 2016) (Fig. 5a). Rounded cobbles and pebbles of beachrock occur on

the seabed in association with this aeolianite (Fig. 5b)., and we thus consider Unit 2.1 to represent a submerged shoreline represented by an aeolianite and beachrock complex.

The tendency of the chaotic reflections of Unit 2.2 to rest in the saddles between the elevated pinnacles of the former barriers (Figs. 6 and 9) and to onlap the landward and seaward faces of the barrier complexes (Figs. 6-9), as well as its propensity to thin laterally away from these barriers (Figs. 6 and 9), suggests a close association between the two. Green et al. (2018) and Cooper et al. (2019) examined rocky beachrock and aeolianite platforms from modern coastlines where weathered and collapsed blocks of beachrock and aeolianite have been reworked by storms to abut both the landward and seaward edges of the shorelines, forming washover fans and collapse aprons. We consider Unit 2.2 to be the equivalent; a residual deposit of aeolianite rubble, derived from the weathering and subsequent reworking of the palaeo-shoreline during rising sea level after lithification. This material was deposited within the hollows between confinement points created by the aeolianite barriers.

5.1.3. Transgressive marine sand sheet

Based on the flat-lying and parallel seismic reflection configuration of Unit 4, and its position above the subaerial unconformity and below a large-scale prograding shelf clinof orm (Figs. 3, 8 and 9), we interpret this as a transgressive marine sand sheet. This is in keeping with similar interpretations by Liu et al. (2004) for the Yellow River's submerged delta, in addition to other similar shelf sediment bodies in Spain (Hernandez-Molina et al., 2000; Lobo et al., 2001), as well as on the west (Kirkpatrick et al., 2019) and east coasts (Dyer et al., 2021) of southern Africa. Its presence is attributed to the deltaic setting and its irregular distribution and variable thickness to bedrock topography and accommodation space.

5.1.4. Proximal and distal delta facies

Units 5 and 6 comprise the thickest accumulations of sediment on the shelf. Engelbrecht et al. (2020) previously recognised these units as consecutive phases of delta construction and outbuilding during periods of relative sea-level stability between -40 and -32 m (Figs. 3, 6 and 7). We now recognise the further seaward extension of these deltaic units beyond two previously undocumented basement highs at -20 m (Fig. 6) and -30 to 40 m (Fig. 7, 8 and 9) that separate two distinct depocenters (proximal and central) (Fig. 4). The delta toe abuts the -60 m shoreline in some places, with occasional lobes to seaward. A third and less pronounced basement high occurs on the outer shelf (Fig. 3), seaward of which a third and smaller (< 10 m-thick) distal depocenter of Unit 5 and 6 occurs (Fig. 4). This distal depocenter abuts the -95 m shoreline to seaward with the rollover depth of the delta clinoform at -55 to -60 m (Figs. 3 and 9).

Unit 6 comprises comparatively finer grain sizes (silt to medium sand) compared to the predominantly coarser grained (medium sand to very coarse-grained sand) material of the deltas of Unit 5. This relative fining may represent:

- i) A finer grained equivalent of the underlying delta, the result of lowered fluvial competencies due to base level rise;
- ii) Backstepping of the deltas, with Unit 6 representing a more distal delta facies such as the prodelta; or
- iii) A combination of the above. As the delta is translated landwards, fluvial competencies are lowered, and a more distal portion of the delta overlies the more proximal delta front facies. Engelbrecht et al. (2020) suggested that the lower unit

equated to a proximal delta front facies (Unit 5) overlain by the more distal prodelta facies (Unit 6) on the inner Thukela shelf.

5.1.6. Relict shoreface sediments and the contemporary mud cliniform

The landward migration of the wave base and the shoreline during the most recent postglacial transgression is marked by wRS, which is interpreted as the wave ravinement based on its seismic and lithological characteristics (Fig. 10). The overlying sediments on the mid-to outer-shelf constitute older shoreface materials that have been prevented from landward migration and dammed seaward of the -60 m shoreline.

This sediment takes the form of asymmetrical southward migrating bedforms (slip faces oriented south), with their form and location suggesting they may have originated as a series of shoreface-connected ridges associated with the -60 m shoreline. The deeper sections of these bedforms exhibit wavelengths (250-600 m) that closely resemble modern shoreface-connected ridges (Guerrero et al., 2018). The shallower sections of these bedforms have likely experienced current reworking on the modern shelf. Unit 7 is therefore considered to represent the partially or incompletely reworked surface expression of overstepped shoreface-connected ridges from the 60 m palaeo-shoreline as per the models of Nnafie et al. (2014) where, as a consequence of a retreating shoreface, new ridges appear on the new part of the inner shelf, while growth of old ridges that were formed on the antecedent part, weakens and they drown over time. In the proximal areas, the shoreface is now represented by the muddy sediments of Unit 8 which constitute the contemporary muddy prodelta of the Thukela River (Engelbrecht et al., 2020).

5.2 Seafloor Morphology

5.2.1 Palaeo-shorelines and associated features

The aeolianites and beachrocks of Unit 2.1 crop out to form complex seabed topography, with thickly-developed aeolianites preserved as linear seabed features (Fig. 11). This is especially so for the -60 m shoreline. However, at the shelf edge, the -95 m shoreline forms a linear seaward aeolianite barrier, but with a subdued and lower elevation zone to landward in which the low-lying topography is segmented by cusped forms. These features are akin to the segmenting cusped spits of the coastal waterbodies of the SE African coastal plain (Wright et al., 2000; Green et al., 2022; Dladla et al., 2022). Isolated small channels enter the system. In the northern parts of the preserved waterbody, a series of prograded arcuate spits occur in the back barrier, the geometry of which suggests incremental shallowing that accompanied the segmentation.

Fronting some of the aeolianite ridges are flat erosional surfaces at depths of ~95 m and ~65 m, which correspond with outcrop of wRS (Fig. 12 c and d) and are thus products of wave ravinement of the underlying rocky material. We consider these to be palaeo-rock shore platforms cut into the underlying Pliocene-age siltstones, and which may have formed contemporaneously with the aeolianite ridges to landward, during periods of sea level stability or slowly rising sea levels (e.g. Salzmann et al., 2013).

5.3 General discussion

5.3.1 Shelf evolution, deltas, shorelines and preservation

Figure 13 provides a schematic model for the development of the shelf stratigraphy and morphology. The Thukela shelf has been subaerially exposed several times during the

Pleistocene, most notably during lowstands deeper than the -100 m shelf break (Fig. 2). Several authors (Green and Garlick, 2011; Cawthra et al., 2012; Pretorius et al., 2019) have identified a prominent erosional surface superimposed on the uppermost portions of the SE African shelf that extends to depths associated with the Pleistocene lowstands highlighted in figure 2. This surface (SB1 of this study) is likely the result of several cycles of sea-level fall since MIS 16. Its position marks the upper bedrock surface and dictates the bedrock control on accommodation available during ensuing transgressive deposition (Fig. 13a). The wide and shallow shelf gradient exacerbates shelf grading at lowstand due to the tendency for meandering river courses to develop in low-gradient settings (Xie et al., 2019), and due to the overall limited accommodation provided by the shallower shelf compared to steeper examples (e.g. Green, 2011; Salzmann et al., 2013).

The oldest units that are identified above this surface, and which are not associated with incised valley deposits, comprise the shoreline complexes (Fig. 13b and c) and delta deposits. On the outer Thukela shelf, a palaeo-shoreline with preserved lagoons at -105 m correlates well with periods of sea level stability around that depth that both predate and postdate the LGM (Fig. 2) (Ishiwa et al., 2019). In total, these stillstands equate to ~ 3.5 ka of shoreline occupation at that depth (Fig. 2).

A second palaeo-shoreline at ~-60 m has been linked to the Younger Dryas cooling event (12.7 ka BP – 11.6 ka BP), identified both regionally (Salzmann et al., 2013; Pretorius et al., 2016) and globally (Locker et al., 1996). The most distal delta has a rollover of ~ 60 m depth and we regard the timing of delta formation as co-eval with the -60 m shoreline.

A third barrier system at -40 m coincides with the formation of the central delta depocenter at similar depths (Fig. 13e) (Engelbrecht et al., 2020). The delta's development was related to a slowstand during which sea-level rose from -46 m to -42 m between 11.5 and 10.6 cal ka BP. This interval coincides temporally with the development of the Yellow River subaqueous delta ~11–9.2 ka BP at similar depths (42 to 38 m, Liu et al., 2004), and which was linked to increased discharge and sediment loads of several other Asian rivers including the Yangtze, G-B, Indus and Mekong (Chen et al., 2000; Goodbred and Kuehl, 2000; Prins and Postma, 2000; Ta et al., 2002). While we have no data to corroborate an increase in palaeo-fluvial discharge in the study area's hinterland, barrier development at this depth and time matches regional examples from the Durban (Pretorius et al., 2016) and southern Mozambican shelf (De Lecea et al., 2017), as well as elsewhere in the world (Storms et al., 2008). The inner proximal delta depocenter was linked to a slowstand between 10.1 to ≤ 9 cal ka BP (Engelbrecht et al., 2020).

Preservation of the -105 m and -60 m barrier systems can relate to rapid drowning of the shoreline form, preserving the features in situ, or due to initially large volumes of material with a significant inertia to overcome during shoreline translation (Cooper et al., 2018a). Rapid rises in sea level have been linked to periods of catastrophic ice sheet collapse associated with MWP-1A (14.3 ka BP - 12.8 ka BP), MWP-1B (11.5 ka BP - 11.2 ka BP) and MWP-1C (9.8 and 9 ka BP), respectively (Deschamps et al., 2012; Green et al., 2014; Abdul et al., 2016; Pretorius et al., 2016, 2019). The evidence for relict parabolic dunes, barrier-lagoon systems and other sandy shorelines indicates significant sediment volumes in the shoreline during transgression. Using a modelling approach, Ciarletta et al. (2019) show that some barriers develop partial autogenic overstepping on slopes of less than 0.17° and under relatively conservative rates of sea level rise. However, despite the general shelf slope being relatively flat, the antecedent

slope provided by the underlying bedrock framework is never less than 0.25° and 0.5° for the area associated with the -60 and -105 m barriers.

Regardless of the mechanism of shoreline preservation, these shoreline sequences have sequestered large volumes of transgressive marine sediment on the shelf through a combination of (i) early lithification (locking sediment into lithified units and the development of aeolianites and beachrocks (e.g. Cooper, 1991) and (ii) physical blocking of the landward transport of shoreline and shoreface sediment (e.g. Anthony and Aagaard, 2020).

Although the depths and timing of shoreline and delta depocenters can be explained by the interplay of sea level rise and sedimentation rates, the spatial variability in the preservation of palaeo-shorelines and delta depocenters documented here demands consideration of other factors.

The degree to which overstepped barriers and deltas are degraded in the nearshore zone during overstepping is believed to be enhanced by factors such as coarser grain-sizes (Mellet et al., 2012), early cementation of the barrier form (Green et al., 2018) and shelf gradient (Storms et al., 2008). The gentle overall palaeo-bathymetric gradient of the Thukela shelf aided in relatively rapid shoreline migration over the shelf with a very low-angle shoreline trajectory thus moderating the degree of transgressive erosion. Green et al. (2018) note that barrier shorelines are particularly well preserved on low-gradient subtropical shelves, as they are predisposed to greater levels of shoreline stability and hence more extensive early cementation. Where steeper zones exist on the palaeo-profile of the Thukela shelf, these are marked by the antecedent high points in the acoustic basement.

A peculiarity of the Thukela shelf is, given the relatively large degree of fluvial sediment supplied to the coastline, and the presence of a subaqueous delta clinoform on the proximal shelf, the remainder of the delta is preserved only as isolated remnants across the shelf, rather than as a continuous single sediment body (Fig. 13e and f). The positioning and form of these patchy deltaic accumulations are constrained by two prominent antecedent features of the shelf. The first overarching control on the spatial distribution of the delta is the basement geology itself. The elevated portions of bedrock have acted as zones of sediment bypass, and deltaic sediments settled seaward of these prominent basement features in the available accommodation (Fig. 4). Though sea level may have been stable and sediment discharge high, delta development and preservation can only occur where the bedrock elevation is comparatively subdued. To landward, these bedrock highs also acted as a physical barrier to delta progradation thus impounding sediments, and encouraging aggradation and thick accumulations that abut the elevated bedrock.

Further impoundment and preservation of the delta units relate to the aeolianite shoreline complexes, which similarly restricted the outbuilding of a continuous deltaic body (Fig. 13e). These ridges created a damming effect along their landward lee, restricting the basinward dispersal of fluvial sediment (e.g. Wenau et al., 2020). The landward flanks of the aeolianites at -105 m and -60 m coincide with the thickest accumulations of deltaic Units 5 and 6. We consider a genetic link between the former shorelines and the associated episodes of delta construction, akin to that observed by Dyer et al. (2021), who identified these palaeo-shorelines as antecedent features around which the delta front prograded via lowpoints or where the barriers were not preserved.

With regards to the shallower delta sequence (Figs. 6-8), the depocenter coincides with a depression in the underlying bedrock in which the initial accommodation for the deltaic bodies was provided (e.g. Engelbrecht et al., 2020) (Fig. 13f). When coupled with the damming of sediment to landward by aeolianite complex (Figs. 3 and 9), this has fostered a substantially thick accumulation of sediment that again has helped buffer transgressive erosion due to the volume of the initial sediment pile (e.g. Cooper et al., 2018b). The landward location of the aeolianite palaeo-shoreline also mediates the shoreline trajectory over the areas in its lee, thus providing preferential preservation as the ravinement profile steps up and over the aeolianite. The combination of shelf gradient, bedrock framework and the mediation of erosion associated with the geologically-controlled shoreline trajectory thus not only control the distribution of delta sediment, but also its preservation.

5.3.2 Primary controls on shoreface sequestration and preservation

The influence of shelf geology on the sedimentary and morphological characteristics of the modern shoreface has been well documented (Riggs et al., 1995; Kirkpatrick and Green, 2018; Menier et al., 2019). While stranded remnants of shoreface on the mid to outer shelf can be simply explained by the inability to “keep pace” with rising sea levels, Cooper et al. (2018b) note that conceptual and analytical models of barrier-shoreface relationships are oversimplified, incomplete or erroneous. These models generally assume the surf-zone-beachface and shoreface migrate in tandem and at the same rates (*sensu* Cowell et al., 1999), however, this investigation shows that geological controls have instead resulted in unusual accumulations of isolated sediment bodies associated with the post-wave ravinement development of the Holocene sediment cover.

On the Thukela shelf, the aeolianites not only sheltered sediment to landward, but acted as a physical impediment to the movement of the shoreface in step with rising sea levels of the last transgression (Fig. 13c and d). The result is an isolated package of shoreface material stranded on the outer portions of the shelf at -105 m, separated from the main shoreface body by more than 60 km and excluded from the modern littoral sediment budget. Likewise, the -60 m barrier acted as a physical impediment to the up-profile translation of the shoreface, with thick post-wave ravinement accumulations stranded on the seaward edge of the barrier (Fig. 6, 7a and 9), and since reworked by the Agulhas Current. The implications are profound for the evolution of coasts with prominent aeolianite bodies. As the shoreline migrates landward with rising sea levels, the sediment budget may become increasingly sediment poor thus promoting shoreline erosion as opposed to roll over. If nearshore geological control is strong, this may result in coastal squeeze and the development of modern rocky shorelines (e.g. Green et al., 2020).

6. Conclusions

This study provides a shelf-wide example of antecedent geology as a primary control on sediment distribution, including that associated with palaeo-shorelines, a wave-dominated delta, and shoreface deposits. Spanning, at the very least, the past 18 000 years, the geological framework of the shelf has repeatedly acted as an overarching control on the sediment dynamics, and the resultant coastal features, now preserved on the seabed.

The three major antecedent geological controls on a wave-dominated delta and coast during transgression are as follows:

- 1) Basement topography underpins the spatial distribution of sediments, being an overarching control in either creating (subaerial unconformity depressions) or limiting (zones of bedrock highs) accommodation space on the shelf.
- 2) Aeolianite ridges control the seaward and landward transference of deltaic sediment, with the damming of sediment on the landward flank associated with capturing of the delta toe, prohibiting basinward outbuilding, while the damming of sediment on the seaward flank is associated with the obstruction of the landward translation of shoreface sediment.
- 3) Shelf gradient facilitates ultimate preservation of coastal features, where gentle shelf gradients allow for rapid landward shoreline translation, especially in the context of MWP. The aeolianite ridges provide steeper points around which the shoreline trajectory is steepened, thus mediating transgressive erosion directly to landward.

Geological control, even in the context of deltaic sequences, thus plays a significant role in the preservation and development of shelf-hosted transgressive stratigraphic sequences, producing unusual distributions of deltaic depocenters and relict shoreface successions.

Acknowledgements

This paper uses data collected through the scientific surveys with the research vessel Dr Fridtjof Nansen as part of the collaboration between the Food and Agriculture Organization of the United Nations (FAO) on behalf of the EAF-Nansen Programme and South Africa. The EAF-Nansen Programme is a partnership between the FAO, the Norwegian Agency for Development Cooperation (Norad), and the Institute of Marine Research (IMR) in Norway for

sustainable management of the fisheries in partner countries and regions. We thank Dr Peter Ramsay and Ian Wright for the legacy vibrocore data, and acknowledge UKZN for a PhD scholarship for LE. Drs Kathrine Michalsen and Sean Fennessy for the opportunity to collect the geophysical data aboard the Nansen.

Data availability

Data are available on reasonable request from the corresponding author, pending permission from the FAO

References

- Abdul, N.A., Mortlock, R.A., Wright, J.D., Fairbanks, R.G., 2016. Younger Dryas sea level and meltwater pulse 1B recorded in Barbados reef crest coral *Acropora palmata*. *Paleoceanography* 31, 330-344.
- Anthony, E.J. and Aagaard, T., 2020. The lower shoreface: Morphodynamics and sediment connectivity with the upper shoreface and beach. *Earth-Science Reviews*, 210, p.103334.
- Besset, M., Anthony, E.J., Bouchette, F., 2019. Multi-decadal variations in delta shorelines and their relationship to river sediment supply: An assessment and review. *Earth-Science Reviews*, 193-199-219.
- Bortolin, E.C., Weschenfelder, J. and Cooper, J.A.G, 2018. Incised valley paleoenvironments interpreted by seismic stratigraphic approach in Patos Lagoon, Southern Brazil. *Brazilian Journal of Geology*, 48, pp.533-551.
- Bosman, C., Uken, R., and Ovechkina, M.N., 2007. The Aliwal Shoal revisited: New age constraints from nannofossil assemblages: *South African Journal of Geology*, v. 110, p. 647–653, doi: 10.2113/gssajg.110.4.647.

Broad, D.S., Jungslager, E.H.A., McLachlan, I.R., Roux, J., 2006. Offshore Mesozoic Basins. In: Johnson, M.R., Anhaeusser, C.R., Thomas, R.J. (Eds.), *The Geology of South Africa*. Geological Society of South Africa, Johannesburg, pp. 553–571 (Council for Geoscience, Pretoria, South Africa).

Camoin, G., Montaggioni, L.F., Braithwaite, C.J.R., 2004. Late glacial to postglacial sea levels in the Western Indian Ocean. *Mar. Geol.* 206, 119-146.

Cawthra, H.C., Uken, R., Ovechkina, M.N., 2012. New insights into the geological evolution of the Durban Bluff and Adjacent Blood Reef, South Africa. *South African Journal of Geology* 115, 291-308.

Chen, Z., Song, B., Wang, Z., and Cai, Y., 2000. Late Quaternary evolution of the sub-aqueous Yangtze Delta, China: sedimentation, stratigraphy, palynology, and deformation: *Marine Geology*, v. 162, p. 423–441, doi: 10.1016/s0025-3227(99)00064-x.

Ciarletta, D.J., Lorenzo-Trueba, J.O.R.G.E. and Ashton, A.D., 2019. Quasi-periodic barrier overstepping. In *Coastal Sediments 2019: Proceedings of the 9th International Conference* (pp. 48-56).

Cooper, J.A.G., 1991. Beachrock formation in low latitudes: implications for coastal evolutionary models. *Marine Geology*, 98(1), pp.145-154.

Cooper, J.A.G. and Flores, R.M., 1991. Shoreline deposits and diagenesis resulting from two Late Pleistocene highstands near+ 5 and+ 6 metres, Durban, South Africa. *Marine Geology*, 97(3-4), pp.325-343.

Cooper, J.A.G., Jackson, D.W.T., Dawson, A.G., Dawson, S., Bates, C.R. and Ritchie, W., 2012. Barrier islands on bedrock: A new landform type demonstrating the role of antecedent topography on barrier form and evolution. *Geology*, 40(10), pp.923-926.

Cooper, J.A.G. and Green, A.N., 2016. Geomorphology and preservation potential of coastal and submerged aeolianite: examples from KwaZulu-Natal, South Africa. *Geomorphology*, 271, pp.1-12.

Cooper, J., Green, A., and Loureiro, C., 2018a. Geological constraints on mesoscale coastal barrier behaviour: *Global and Planetary Change*, v. 168, p. 15–34, doi: 10.1016/j.gloplacha.2018.06.006.

Cooper, J., Green, A., and Compton, J., 2018b. Sea-level change in southern Africa since the Last Glacial Maximum: *Quaternary Science Reviews*, v. 201, p. 303–318, doi: 10.1016/j.quascirev.2018.10.013.

Cooper, J., Green, A., Meireles, R., Klein, A., Abreu, J.D., and Toldo, E., 2019. Tidal strait to embayment: Seismic stratigraphy and evolution of a rock-bounded embayment in the context of Holocene sea level change: *Marine Geology*, v. 415, p. 105972, doi: 10.1016/j.margeo.2019.105972.

Cowell, P.J., Roy, P.S., Cleveringa, J. and De Boer, P.L., 1999. Simulating coastal systems tracts using the shoreface translation model.

De Lecea, A.M., Green, A.N., Strachan, K.L., Cooper, J.A.G., Wiles, E.A., 2017. Stepped Holocene sea-level rise and its influence on sedimentation in a large marine embayment: Maputo Bay, Mozambique. *Estuar. Coast. Shelf Sci.* 193, 25–36. <https://doi.org/10.1016/j.ecss.2017.05.015>.

Deschamps, P., Durand, N., Bard, E., Hamelin, B., Camoin, G., Thomas, A.L., Henderson, G.M., Okuno, J.I., Yokoyama, Y., 2012. Ice-sheet collapse and sealevel rise at the Bølling warming 14,600 years ago. *Nature* 483, 559.

Dingle, R.V., Scrutton, R.A., 1974. Continental break-up and the development of postPalaeozoic sedimentary basins around southern Africa. *Geological Society of America Bulletin* 85, 1467–1474.

Dingle, R.V., Siesser, W.G., Newton, A.R., 1983. *Mesozoic and Tertiary Geology of Southern Africa*. AA Balkema, Rotterdam, p. 375.

Dladla, N.N., Green, A.N., Humphries, M.S., Cooper, J.A.G., Godfrey, M. and Wright, C.I., 2022. Back-barrier evolution and along-strike variations in infilling of the Kosi Bay lake system, South Africa. *Estuarine, Coastal and Shelf Science*, 272, p.107877.

Dyer, S.E., Green, A.N., Cooper, J.A.G., Hahn, A. and Zabel, M., 2021. Response of a wave-dominated coastline and delta to antecedent conditioning and fluctuating rates of postglacial sea-level rise. *Marine Geology*, 434, p.106435.

Engelbrecht, L., Green, A.N., Cooper, J.A.G., Hahn, A., Zabel, M. and Mackay, C.F., 2020. Construction and evolution of submerged deltaic bodies on the high energy SE African

coastline: the interplay between relative sea level and antecedent controls. *Marine Geology*, 424, p.106170.

Flemming, B.W., 1978. Underwater sand dunes along the southeast African continental margin—observations and implications. *Marine Geology* 26, 177-198.

Flemming, B.W., 1981. Factors controlling shelf sediment dispersal along the southeast African continental margin. *Marine Geology* 42, 259–277.

Flemming, B.W., 1988. Zur klassifikation subaquatischer, strömungstransversaler Transportkörper. *Bochumer geologische und geotechnische Arbeiten*, 29(93-97), pp.44-47.

Fleming, B., and Hay, R., 1988. Sediment distribution and dynamics on the Natal continental shelf: Lecture Notes on Coastal and Estuarine Studies Coastal Ocean Studies Off Natal, South Africa, p. 47–80, doi: 10.1029/ln026p0047.

Gal, N.S., Wallace, D.J., Miner, M.D., Hollis, R.J., Dike, C. and Flocks, J.G., 2021. Influence of antecedent geology on the Holocene formation and evolution of Horn Island, Mississippi, USA. *Marine Geology*, 431, p.106375.

Gardner, J.V., Dartnell, P., Mayer, L.A., Clarke, J.H., Calder, B.R. and Duffy, G., 2005. Shelf-edge deltas and drowned barrier–island complexes on the northwest Florida outer continental shelf. *Geomorphology*, 64(3-4), pp.133-166.

Gardner, J., Calder, B., Clarke, J.H., Mayer, L., Elston, G., and Rzhanov, Y., 2007. Drowned shelf-edge deltas, barrier islands and related features along the outer continental shelf north of the head of De Soto Canyon, NE Gulf of Mexico: *Geomorphology*, v. 89, p. 370–390, doi: 10.1016/j.geomorph.2007.01.005.

Goodbred, S., and Kuehl, S., 2000. The significance of large sediment supply, active tectonism, and eustasy on margin sequence development: Late Quaternary stratigraphy and evolution of the Ganges–Brahmaputra delta: *Sedimentary Geology*, v. 133, p. 227–248, doi: 10.1016/s0037-0738(00)00041-5.

Goodlad, S.W., 1986. Tectonic and sedimentary history of the mid-Natal valley (SW Indian Ocean): *Bulletin of the Joint Geological Survey of South Africa/University of Cape Town/Marine Geoscience Unit, Council for Geoscience*, v. 15, p. 415.

Green, A., 2011. The late Cretaceous to Holocene sequence stratigraphy of a sheared passive upper continental margin, northern KwaZulu-Natal, South Africa. *Marine Geology*, 289(1-4), pp.17-28.

Green, A.N., Garlick, G.L., 2011. A sequence stratigraphic framework for a narrow, current-swept continental shelf: the Durban Bight, central KwaZulu-Natal, South Africa. *Journal of African Earth Sciences* 60, 303–314.

Green, A.N., Cooper, J.A.G., Leuci, R., and Thackeray, Z., 2013a. Formation and preservation of an overstepped segmented lagoon complex on a high-energy continental shelf: *Sedimentology*, v. 60, p. 1755–1768, doi: 10.1111/sed.12054.

Green, A.N., Dladla, N., and Garlick, G.L., 2013b. Spatial and temporal variations in incised valley systems from the Durban continental shelf, KwaZulu-Natal, South Africa: *Marine Geology*, v. 335, p. 148–161, doi: 10.1016/j.margeo.2012.11.002.

Green, A.N., Cooper, J.A.G., and Salzmann, L., 2014. Geomorphic and stratigraphic signals of postglacial meltwater pulses on continental shelves: *Geology*, v. 42, p. 151–154, doi: 10.1130/g35052.1.

Green, A., and Mackay, C., 2016. Unconsolidated sediment distribution patterns in the KwaZulu-Natal Bight, South Africa: the role of wave ravinement in separating relict versus active sediment populations: *African Journal of Marine Science*, v. 38, doi: 10.2989/1814232x.2016.1145138.

Green, A.N., Cooper, J.A.G., and Salzmann, L., 2018. The role of shelf morphology and antecedent setting in the preservation of palaeo-shoreline (beachrock and aeolianite) sequences: the SE African shelf: *Geo-Marine Letters*, v. 38, p. 5–18, doi: 10.1007/s00367-017-0512-8.

Green, A.N., Cooper, J.A.G., Dlamini, N.P., Dladla, N.N., Parker, D., Kerwath, S.E., 2020. Relict and contemporary influences on the postglacial geomorphology and evolution of a current swept shelf: the Eastern Cape Coast, South Africa. *Mar. Geol.* 427, 106230. <https://doi.org/10.1016/j.margeo.2020.106230>.

Green, A.N., Humphries, M.S., Cooper, J.A.G., Strachan, K.L., Gomes, M. and Dladla, N.N., 2022. The Holocene evolution of Lake St Lucia, Africa's largest estuary: *Geological*

implications for contemporary management. *Estuarine, Coastal and Shelf Science*, 266, p.107745.

GründlIngh, M.L., 1992. Agulhas Current meanders: review and case study. *South African geographical journal*, 74(1), pp.19-28.

Guerrero, Q., Guillén, J., Durán, R. and Urgeles, R., 2018. Contemporary genesis of sand ridges in a tideless erosional shoreface. *Marine Geology*, 395, pp.219-233.

Hernández-Molina, F.J., Somoza, L., and Lobo, F., 2000. Seismic stratigraphy of the Gulf of Cádiz continental shelf: a model for Late Quaternary very high-resolution sequence stratigraphy and response to sea-level fall: Geological Society, London, Special Publications, v. 172, p. 329–362, doi: 10.1144/gsl.sp.2000.172.01.15.

Hicks, N., and Green, A., 2016. Sedimentology and depositional architecture of a submarine delta-fan complex in the Durban Basin, South Africa: *Marine and Petroleum Geology*, v. 78, p. 390–404, doi: 10.1016/j.marpetgeo.2016.09.032.

Ishiwa, T., Yokoyama, Y., Okuno, J.I., Obrochta, S., Uehara, K., Ikehara, M. and Miyairi, Y., 2019. A sea-level plateau preceding the Marine Isotope Stage 2 minima revealed by Australian sediments. *Scientific reports*, 9(1), pp.1-8.

Kirkpatrick, L.H., and Green, A.N., 2018. Antecedent geologic control on nearshore morphological development: The wave dominated, high sediment supply shoreface of southern Namibia: *Marine Geology*, v. 403, p. 34–47, doi: 10.1016/j.margeo.2018.05.003.

Kirkpatrick, L.H., Green, A.N., and Pether, J., 2019. The seismic stratigraphy of the inner shelf of southern Namibia: The development of an unusual nearshore shelf stratigraphy: *Marine Geology*, v. 408, p. 18–35, doi: 10.1016/j.margeo.2018.11.016.

Lambeck, K., Rouby, H., Purcell, A., Sun, Y., Sambridge, M., 2014. Sea level and global ice volumes from the Last Glacial Maximum to the Holocene. *Proc. Natl. Acad. Sci. U. S. A.* 111, 15296–15303. <https://doi.org/10.1073/pnas.1411762111>.

Liu, J., Milliman, J.D., Gao, S., and Cheng, P., 2004. Holocene development of the Yellow Rivers subaqueous delta, North Yellow Sea: *Marine Geology*, v. 209, p. 45–67, doi: 10.1016/j.margeo.2004.06.009.

- Lobo, F.J., Hern´andez-Molina, F.J., Somoza, L., D´ıaz del R´ıo, V., 2001. The sedimentary record of the post-glacial transgression on the Gulf of Cadiz continental shelf (Southwest Spain). *Mar. Geol.* 178, 171–195. [https://doi.org/10.1016/S0025-3227\(01\)00176-1](https://doi.org/10.1016/S0025-3227(01)00176-1).
- Locker, S.D., Hine, A.C., Tedesco, L.P. and Shinn, E.A., 1996. Magnitude and timing of episodic sea-level rise during the last deglaciation. *Geology*, 24(9), pp.827-830.
- Mallinson, D.J., Smith, C.W., Culver, S.J., Riggs, S.R. and Ames, D., 2010. Geological characteristics and spatial distribution of paleo-inlet channels beneath the outer banks barrier islands, North Carolina, USA. *Estuarine, Coastal and Shelf Science*, 88(2), pp.175-189.
- Martin, A.K., and Flemming, B.W., 1986. The Holocene shelf sediment wedge off the south and east coast of South Africa. *Shelf Sands and Sandstones*: v. 11, p. 27–44.
- Martin, A.K., and Flemming, B.W., 1988. *Physiography, Structure and Geological Evolution of the Natal Continental Shelf: Lecture Notes on Coastal and Estuarine Studies Coastal Ocean Studies off Natal, South Africa*, p. 11–46, doi: 10.1007/978-1-4757-3908-4_2.
- Mcormick, S., Cooper, J.A., and Mason, T.R., 1992. Fluvial Sediment Yield to the Natal Coast: A Review: *Southern African Journal of Aquatic Sciences*, v. 18, p. 74–88, doi: 10.1080/10183469.1992.9631326.
- Mellett, C.L., Hodgson, D.M., Lang, A., Mauz, B., Selby, I., and Plater, A.J., 2012. Preservation of a drowned gravel barrier complex: A landscape evolution study from the north-eastern English Channel: *Marine Geology*, v. 315-318, p. 115–131, doi: 10.1016/j.margeo.2012.04.008.
- Menier, D., Mathew, M., Cherfils, J.B., Ramkumar, M., Estournès, G., Koch, M., Guillocheau, F., Sedrati, M., Goubert, E., Gensac, E. and Le Gall, R., 2019. Holocene sediment mobilization in the inner continental shelf of the Bay of Biscay: Implications for regional sediment budget offshore to onshore. *Journal of Coastal Research*, 88(SI), pp.110-121.
- Milliman, J.D., and Farnsworth, K.L., 2011. *River discharge to the coastal ocean: a global synthesis*: Cambridge, Cambridge University Press.
- Moes, H., and Rossouw, M., 2008. Considerations for the utilization of wave power around South Africa: Workshop on Ocean Energy, Centre for Renewable and Sustainable Energy Studies Abstracts, Stellenbosch, South Africa, 21 February.

Nnafie, A., De Swart, H.E., Calvete, D. and Garnier, R., 2014. Effects of sea level rise on the formation and drowning of shoreface-connected sand ridges, a model study. *Continental Shelf Research* 80, 32-48.

Pretorius, L., Green, A., and Cooper, A., 2016. Submerged shoreline preservation and ravinement during rapid postglacial sea-level rise and subsequent “slowstand”: *Geological Society of America Bulletin*, v. 128, p. 1059–1069, doi: 10.1130/b31381.1.

Pretorius, L., Green, A., Cooper, J., Hahn, A., and Zabel, M., 2019. Outer- to inner-shelf response to stepped sea-level rise: Insights from incised valleys and submerged shorelines: *Marine Geology*, v. 416, p. 105979, doi: 10.1016/j.margeo.2019.105979.

Prins, M.A., and Postma, G., 2000. Effects of climate, sea level, and tectonics unravelled for last deglaciation turbidite records of the Arabian Sea: *Geology*, 28, 375, doi: 10.1130/0091-7613(2000)28<375:eocsla>2.0.co;2.

Ramsay, P.J., 1994. Marine geology of the Sodwana Bay shelf, Southeast Africa. *Marine Geology* 120, 225–247.

Riggs, S.R., Cleary, W.J. and Snyder, S.W., 1995. Influence of inherited geologic framework on barrier shoreface morphology and dynamics. *Marine geology*, 126(1-4), pp.213-234.

SAN (South African Navy), 2018. Tide tables. South African Navy, Simonstown.

Salzmann, L., Green, A., and Cooper, J.A.G., 2013. Submerged barrier shoreline sequences on a high energy, steep and narrow shelf: *Marine Geology*, v. 346, p. 366–374, doi: 10.1016/j.margeo.2013.10.003.

Schumann, E.H., 1988. Physical oceanography off Natal: Lecture Notes on Coastal and Estuarine Studies Coastal Ocean Studies Off Natal, South Africa, p. 101–130, doi: 10.1029/ln026p0101.

Shawler, J.L., Ciarletta, D.J., Connell, J.E., Boggs, B.Q., Lorenzo-Trueba, J. and Hein, C.J., 2021. Relative influence of antecedent topography and sea-level rise on barrier-island migration. *Sedimentology*, 68(2), pp.639-669.

Shepard, F.P., 1963. *Submarine Geology*: New York, Harper and Row, 557 p.

Spratt, R.M., and Lisiecki, L.E., 2015. A late Pleistocene sea level stack. *Climate of the Past Discussions*, 11, 3699-3728.

- Stanford, J.D., Hemingway, R., Rohling, E.J., Challenor, P.G., Medina-Elizalde, M., Lester, A.J., 2011. Sea-level probability for the last deglaciation: a statistical analysis of far-field records. *Global Planet. Change* 79, 193-203.
- Storms, J.E., Weltje, G.J., Terra, G.J., Cattaneo, A. and Trincardi, F., 2008. Coastal dynamics under conditions of rapid sea-level rise: Late Pleistocene to Early Holocene evolution of barrier–lagoon systems on the northern Adriatic shelf (Italy). *Quaternary Science Reviews*, 27(11-12), pp.1107-1123.
- Syvitski, J.P.M., Kettner, A.J., Overeem, I., Hutton, E.W.H., Hannon, M.T., Brakenridge, G.R., Day, J., Vörösmarty, C., Saito, Y., Giosan, L., and Nicholls, R.J., 2009. Sinking deltas due to human activities: *Nature Geoscience*, v. 2, p. 681–686, doi: 10.1038/ngeo629.
- Ta, T., Nguyen, V., Tateishi, M., Kobayashi, I., Tanabe, S., and Saito, Y., 2002. Holocene delta evolution and sediment discharge of the Mekong River, southern Vietnam: *Quaternary Science Reviews*, v. 21, p. 1807–1819, doi: 10.1016/s0277-3791(02)00007-0.
- Vörösmarty, C.J., Syvitski, J., Day, J., Sherbinin, A.D., Giosan, L., and Paola, C., 2009. Battling to Save the World’s River Deltas: *Bulletin of the Atomic Scientists*, v. 65, p. 31–43, doi: 10.2968/065002005.
- Wenau, S., Preu, B. and Spiess, V., 2020. Geological development of the Limpopo Shelf (southern Mozambique) during the last sea level cycle. *Geo-Marine Letters*, 40(3), pp.363-377.
- Wright, C.I., Miller, W.R. and Cooper, J.A.G., 2000. The late Cenozoic evolution of coastal water bodies in Northern Kwazulu-Natal, South Africa. *Marine Geology*, 167(3-4), pp.207-229.
- Xie, Q., Yang, J. and Lundström, T.S., 2019. Field studies and 3D modelling of morphodynamics in a meandering river reach dominated by tides and suspended load. *Fluids*, 4(1), p.15.

Figure captions

Fig. 1: Locality map illustrating the extent of seismic coverage (bold lines corresponding to subsequent figures), core localities (with larger red points correlating to subsequent figures), ROV data and grab samples (Fig.5), and multibeam bathymetry.

Fig. 2: Relative sea level curve for a) the Mid to late Pleistocene derived from Spratt and Lisiecki (2015) and b) the late Pleistocene to Holocene compiled from southern African records (Cooper et al., 2018) and data from the Bonaparte Gulf (Ishiwa et al., 2019). MWP = Meltwater Pulse. Yellow lines refer to the positions of shorelines (deltas and aeolianite/beachrocks) on the Thukela Shelf, red block denotes periods where sea level has fallen below the shelf break.

Fig. 3: Coast perpendicular Topas seismic reflection profile. Inset: Note the washout of underlying reflectors beneath Unit 2.1 and the local positive relief in the sea floor expression where Units 5 and 6 are present.

Fig. 4: a) Isopach map of Post-SB1 sediments and b) SB1 surface elevation relative to mean sea level (MSL).

Fig 5: a) ROV footage of high angle planar foresets forming overhangs in Unit 2.1. b) Grab samples of material immediately adjacent to outcrop of Unit 2.1. Note the pebbles of beachrock. c) plain and d) cross polarised light photomicrographs of beachrocks in association with Unit 2.1. Note the relatively blocky calcite cement. P = peloid, BC = blocky calcite, CR = cryptocrystalline rim, VS = void space, SF = shelf fragment, L = lithic, Q = quartz.

Fig. 6: Coast perpendicular Topas seismic reflection profile with the locality of Cores 21, 22 and 24. Inset: note the very large dune features in the uppermost portions of Unit 7, dammed on the seaward edge of the high relief pinnacles of Unit 2.1 and wRS underlying Unit 7.

Fig. 7: Coast perpendicular Topas seismic reflection profile. Inset a: Bedrock high. Inset b: Unit 2.1 outcrop at the sea floor with major positive relief expression. Unit 7 occurs on the seaward flank of Unit 2.1, with a thick accumulation of Unit 5 distally in the local depression caused by the steepening and outcrop of Unit 1 and the damming of sediment against Unit 2.1 to landward.

Fig. 8: Coast perpendicular Topas seismic reflection profile. Inset: The positive relief in the bedrock surface (Unit 1) where Units 5 and 6 are thickest. Note the truncation by wRS of Units 5 and 6, marking the basal surface of the overlying Unit 8, and the location of Core 23 intersecting Units 5 and 6.

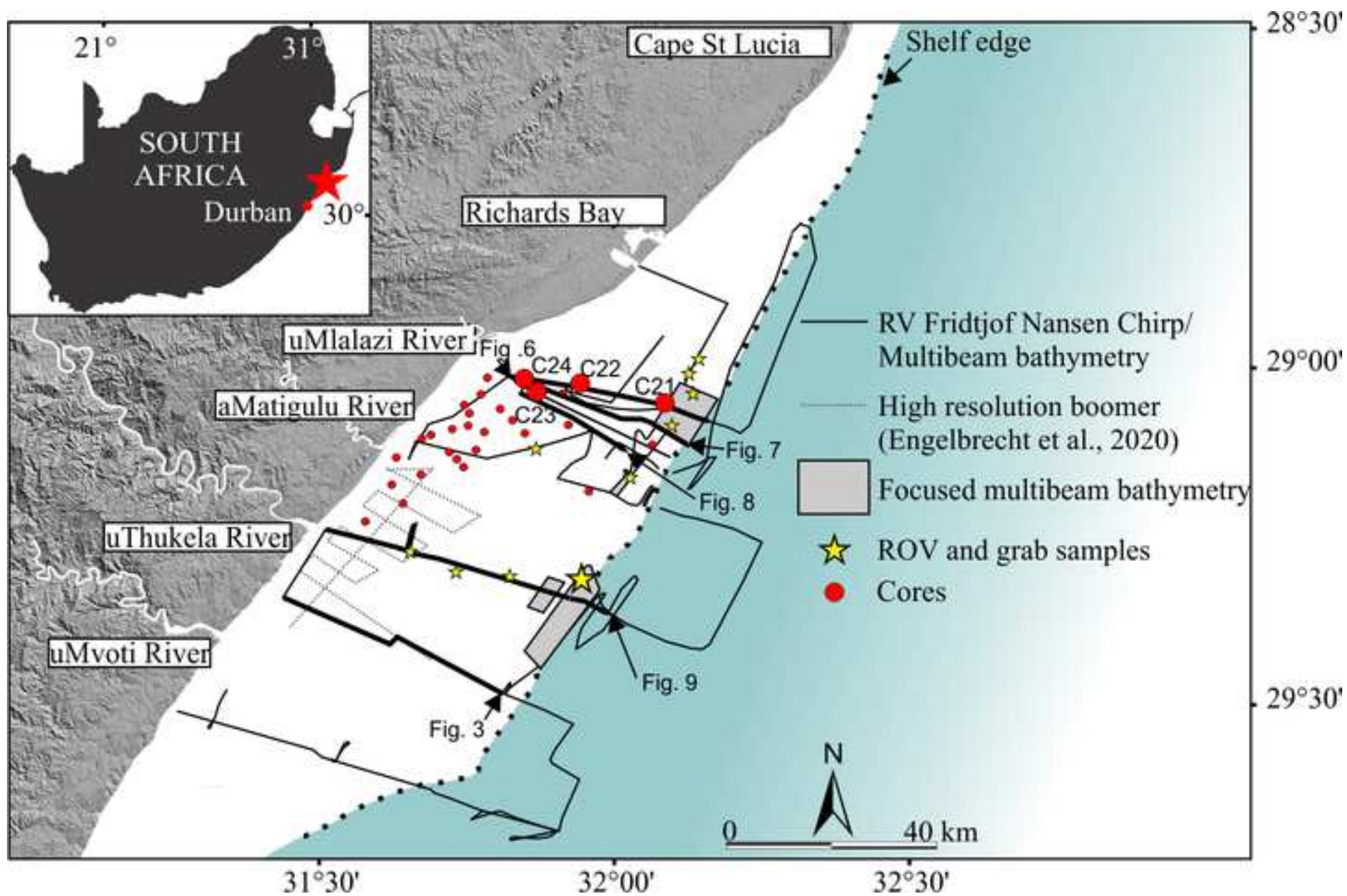
Fig. 9: Coast perpendicular Topas seismic reflection profile. Inset: The positive relief of the seafloor formed by Units 2.1, 5 and 6, and the location of Unit 7 on the seaward edge of Unit 2.1, underlain by the wRS.

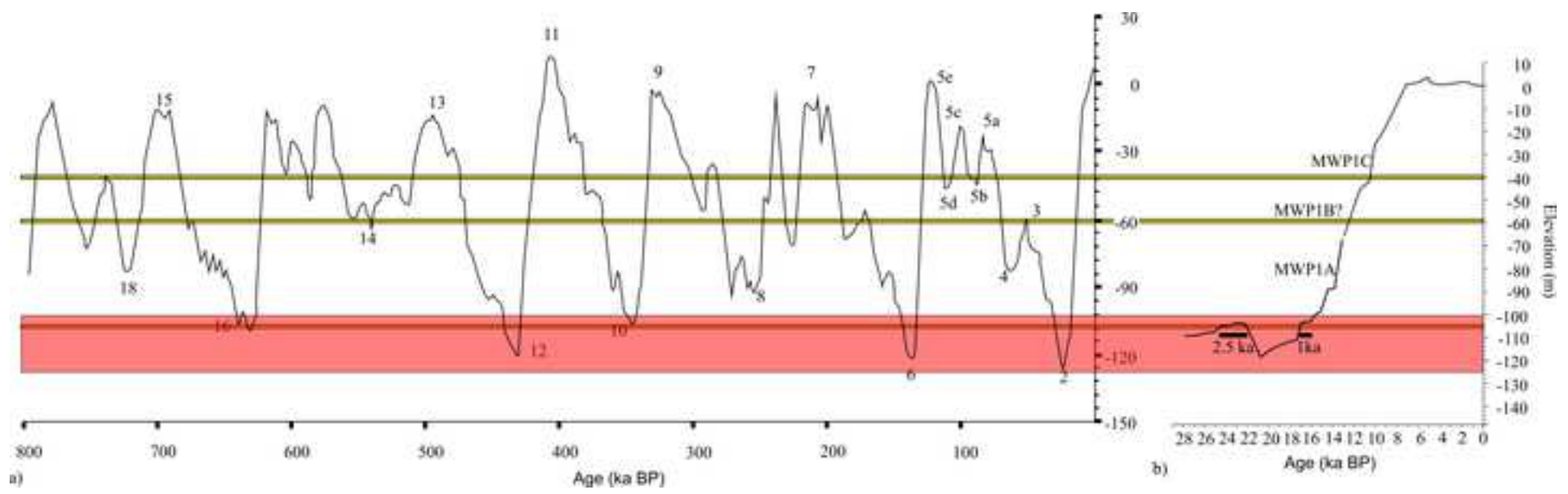
Fig 10: Lithostratigraphy for cores 21 through 24, with seismic profile for locations.

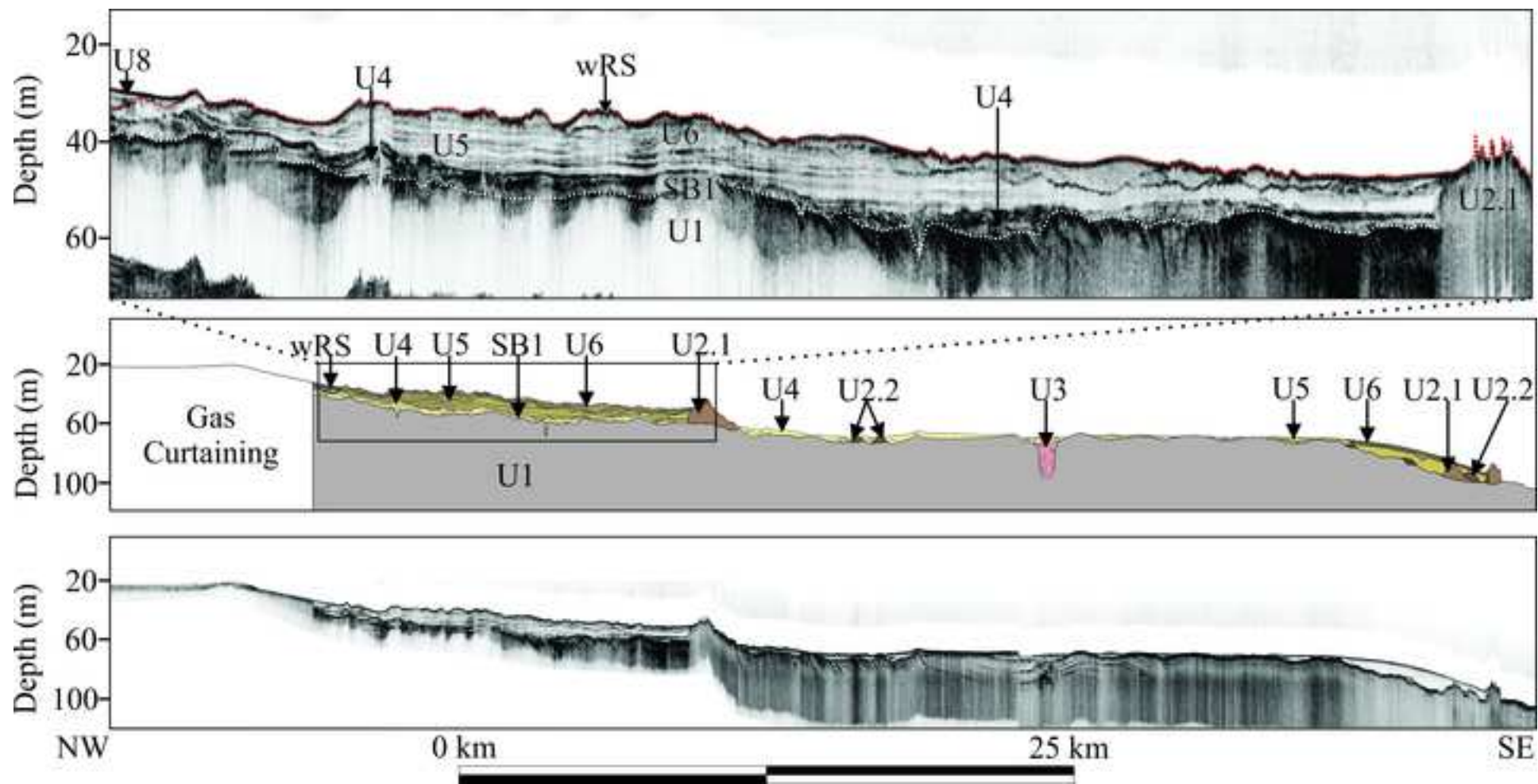
Fig. 11: Multibeam bathymetric maps of the a) southern and b) northern continental shelf revealing raised ridges. The various bathymetric cross sections and close up bathymetry show c) raised parabolic ridges, d) recurved ridges, e) raised ridges fronted by planation surfaces and f) raised ridge at -60 m.

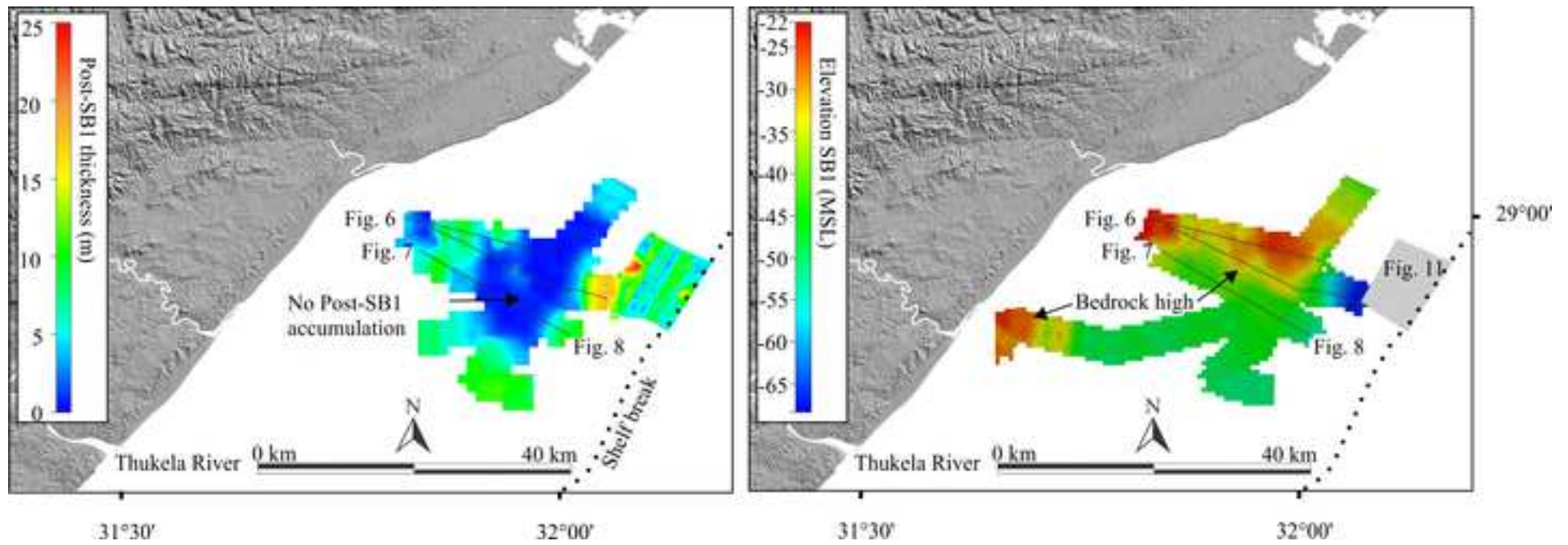
Fig. 12: Isopach maps of aeolianite thickness in a) the southern and b) northern blocks. c) isopach maps of post-wRS sediment in the south and d) north. Note in c) wRS crops out along the seabed, and in d) crops out to landward of the main body of post wRS sediment accumulation.

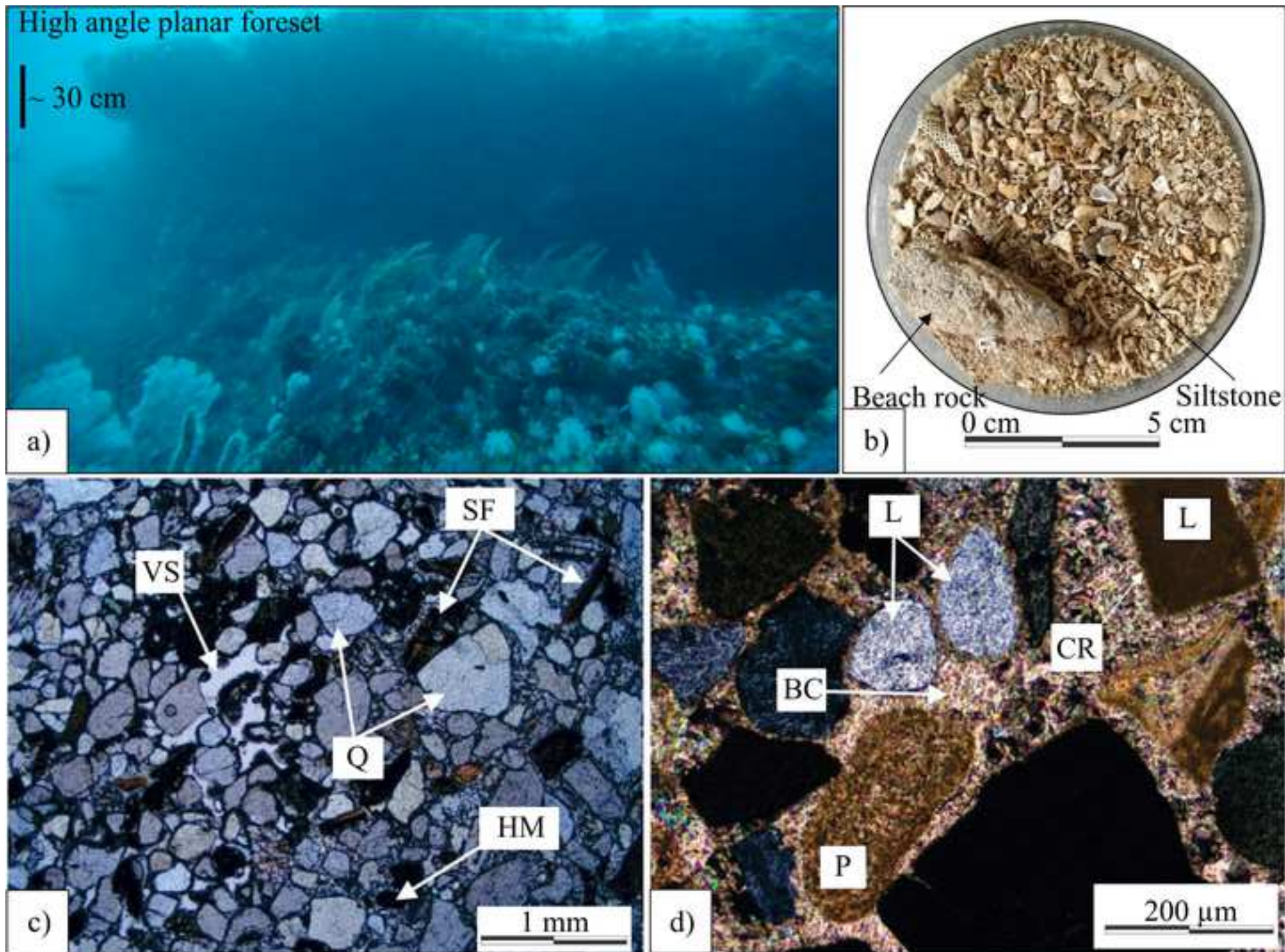
Fig. 13: An evolutionary model for the shelf. a) rivers cross shelf at lowstands, subaerial unconformity develops with associated bedrock highs as interfluves. b) stillstand and development of palaeo-shoreline with lagoons at -100 m. c) sea-level rise strands shoreface at -100 m shoreline. A stillstand at ~ 60 m water depth forms the -60 m shoreline together with outer distal delta, both abutting bedrock high. d) sea-level rises and strands shoreface on the -60 m shoreline, later reworked into subaqueous dune field. e) Stillstand and development of -40 m shoreline, and central delta against bedrock high. f) continued rise in sea level with slowing of rates causes proximal delta to form abutting innermost bedrock high.

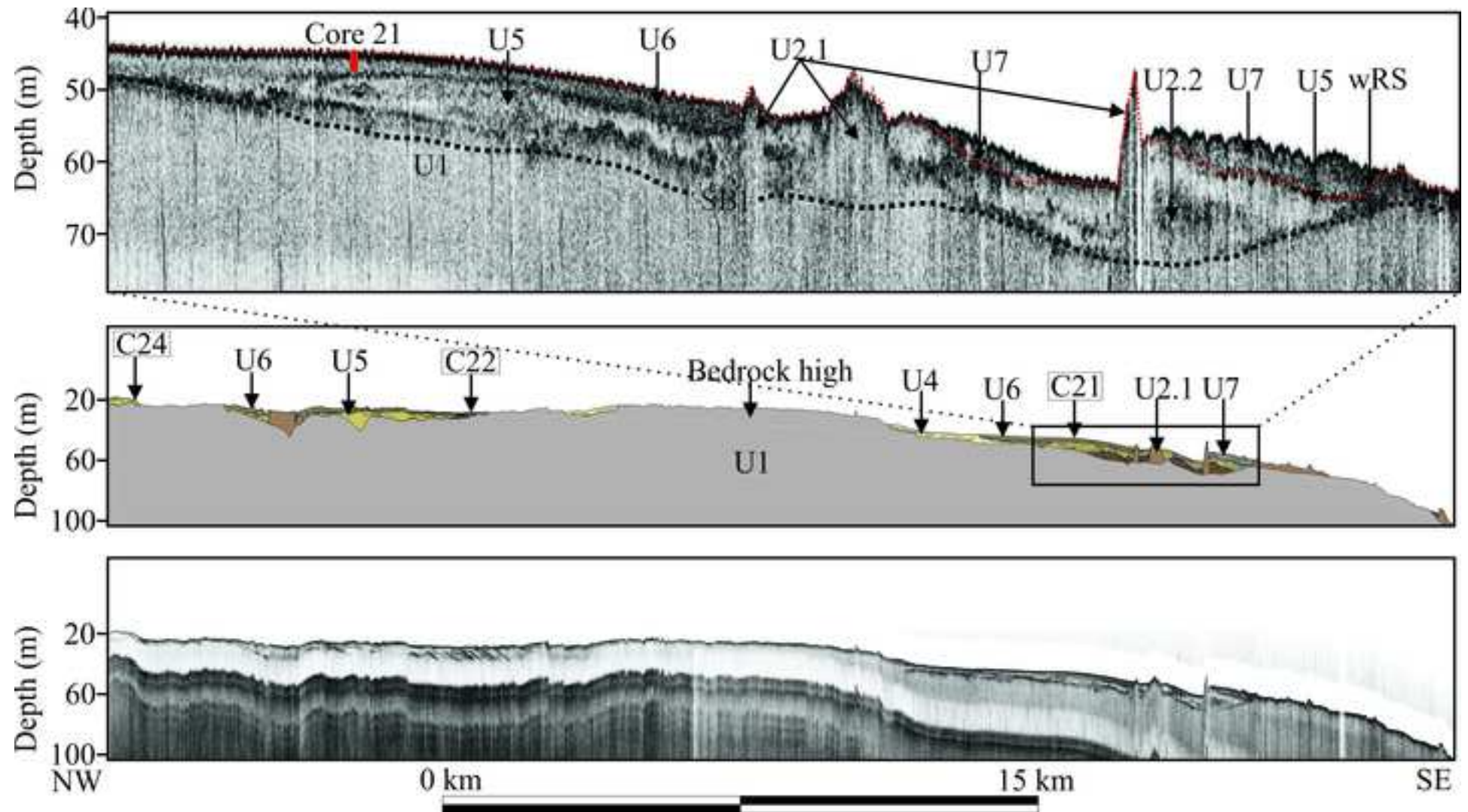


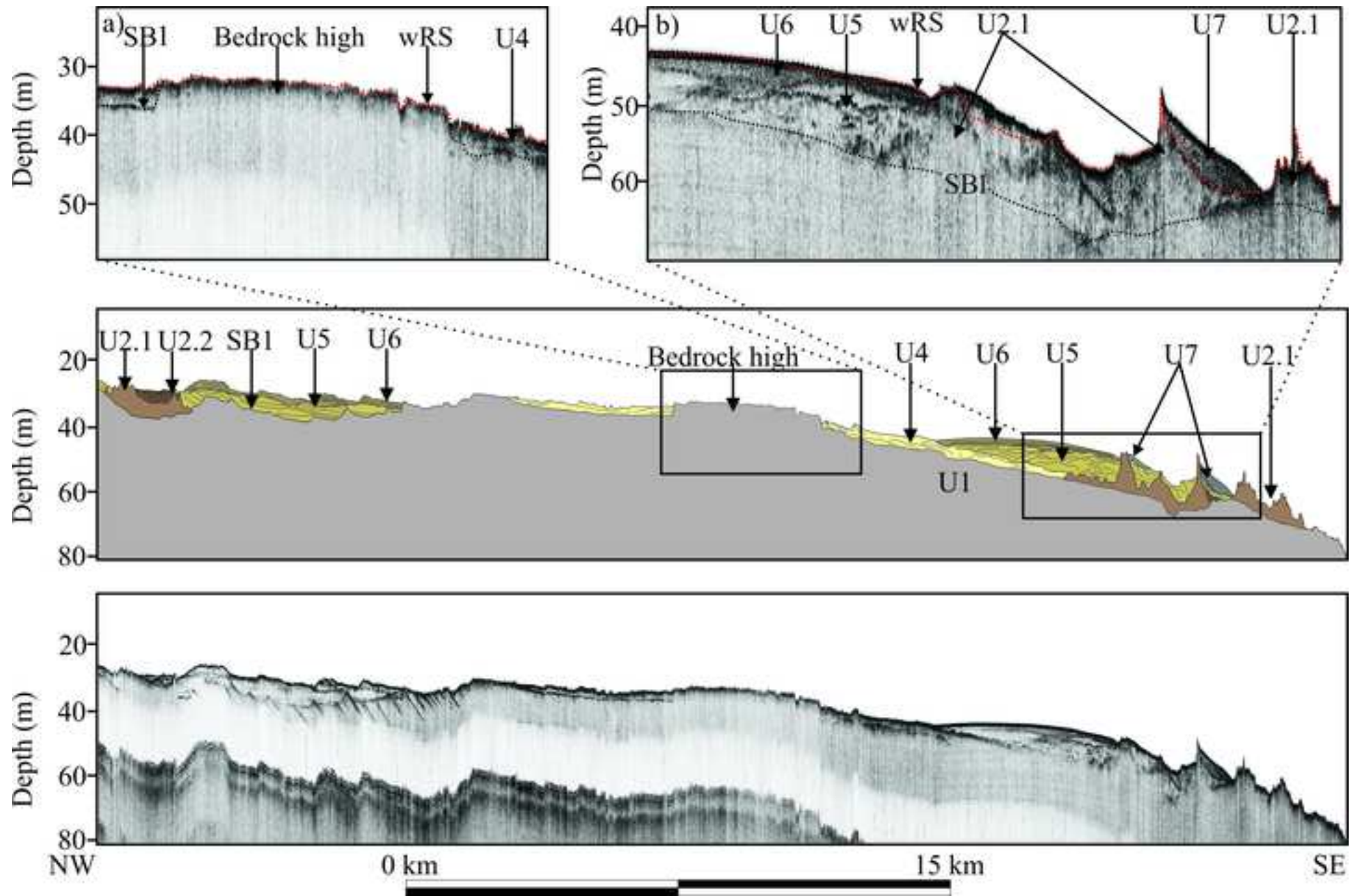


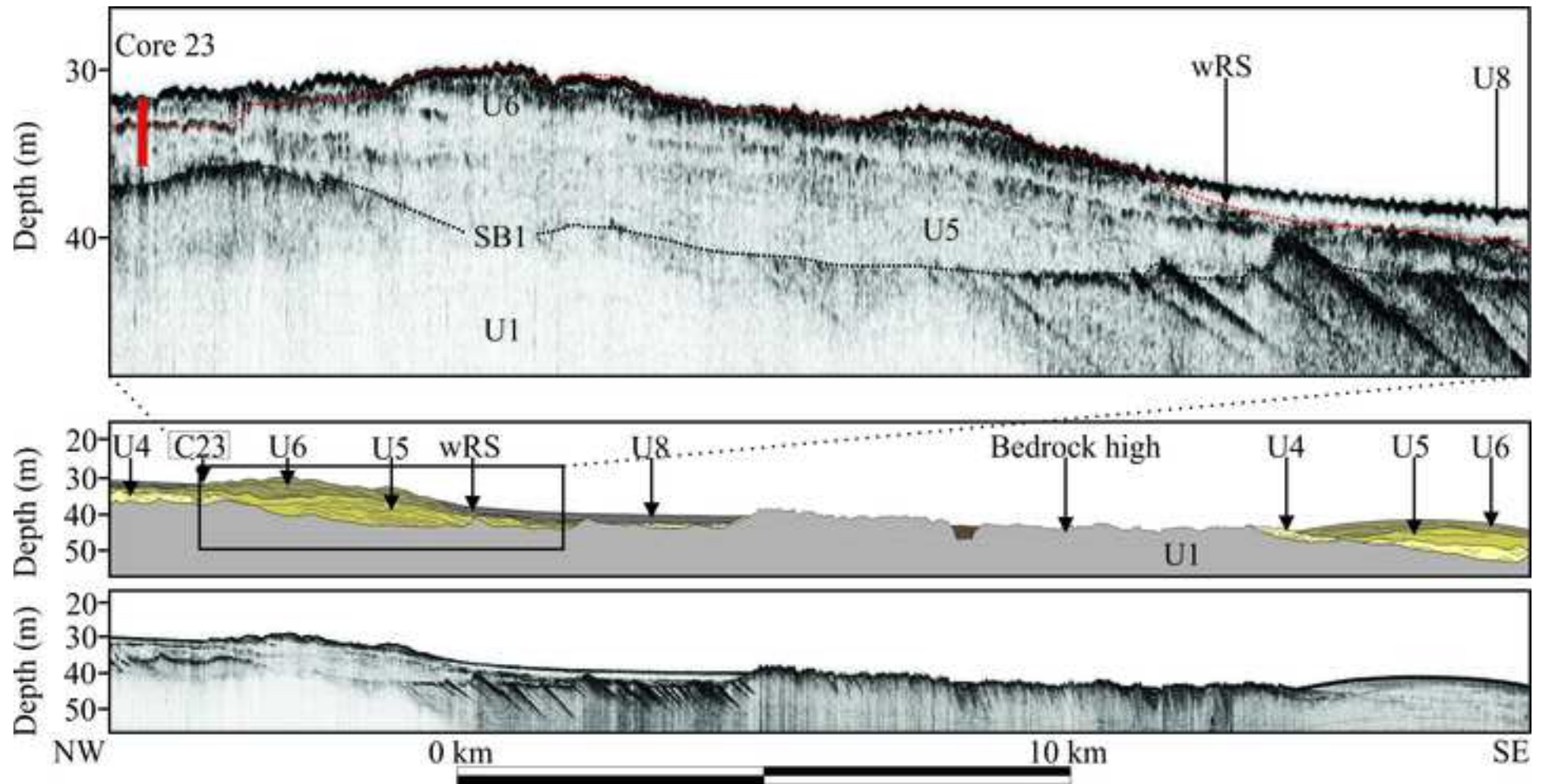


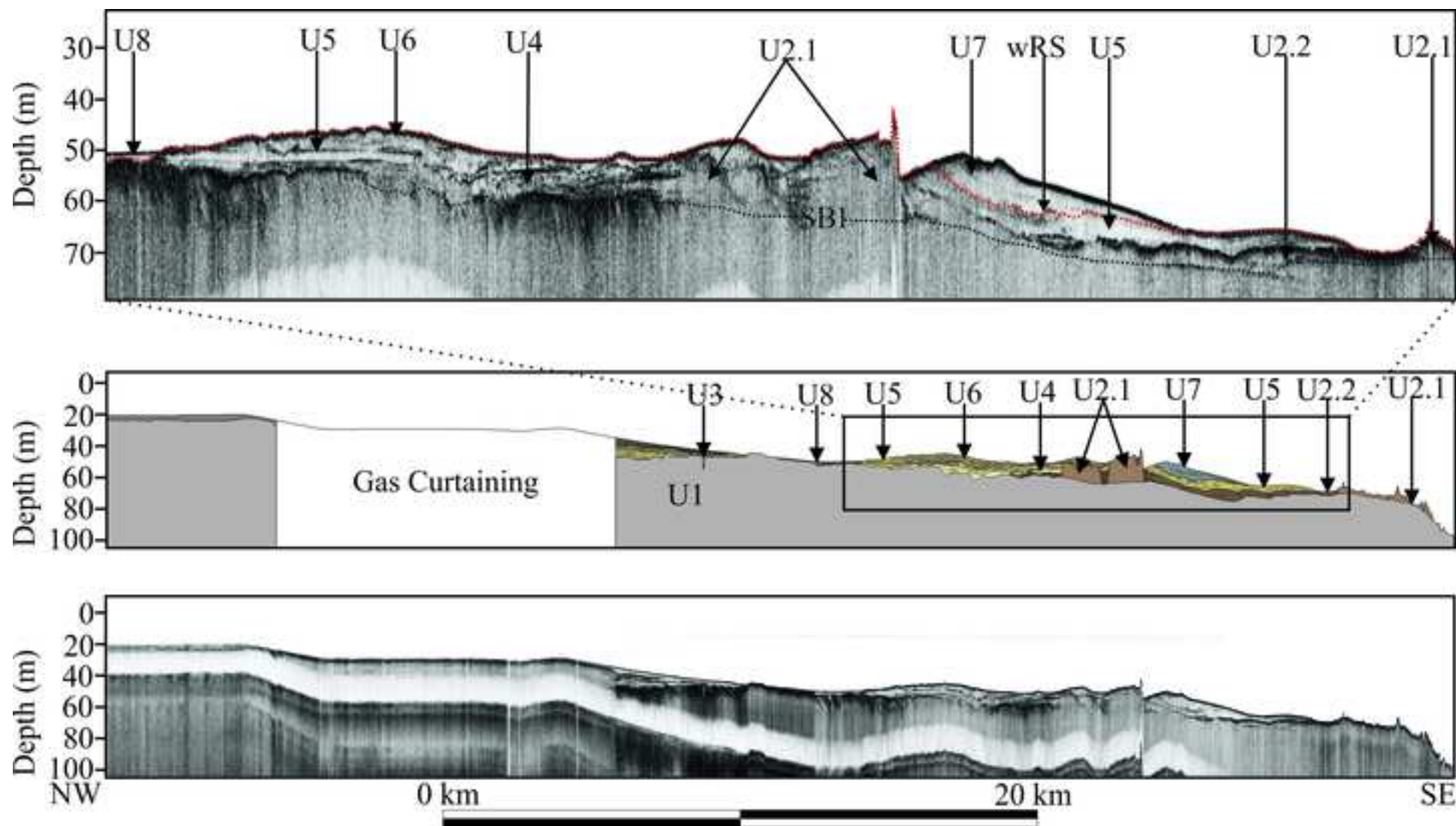


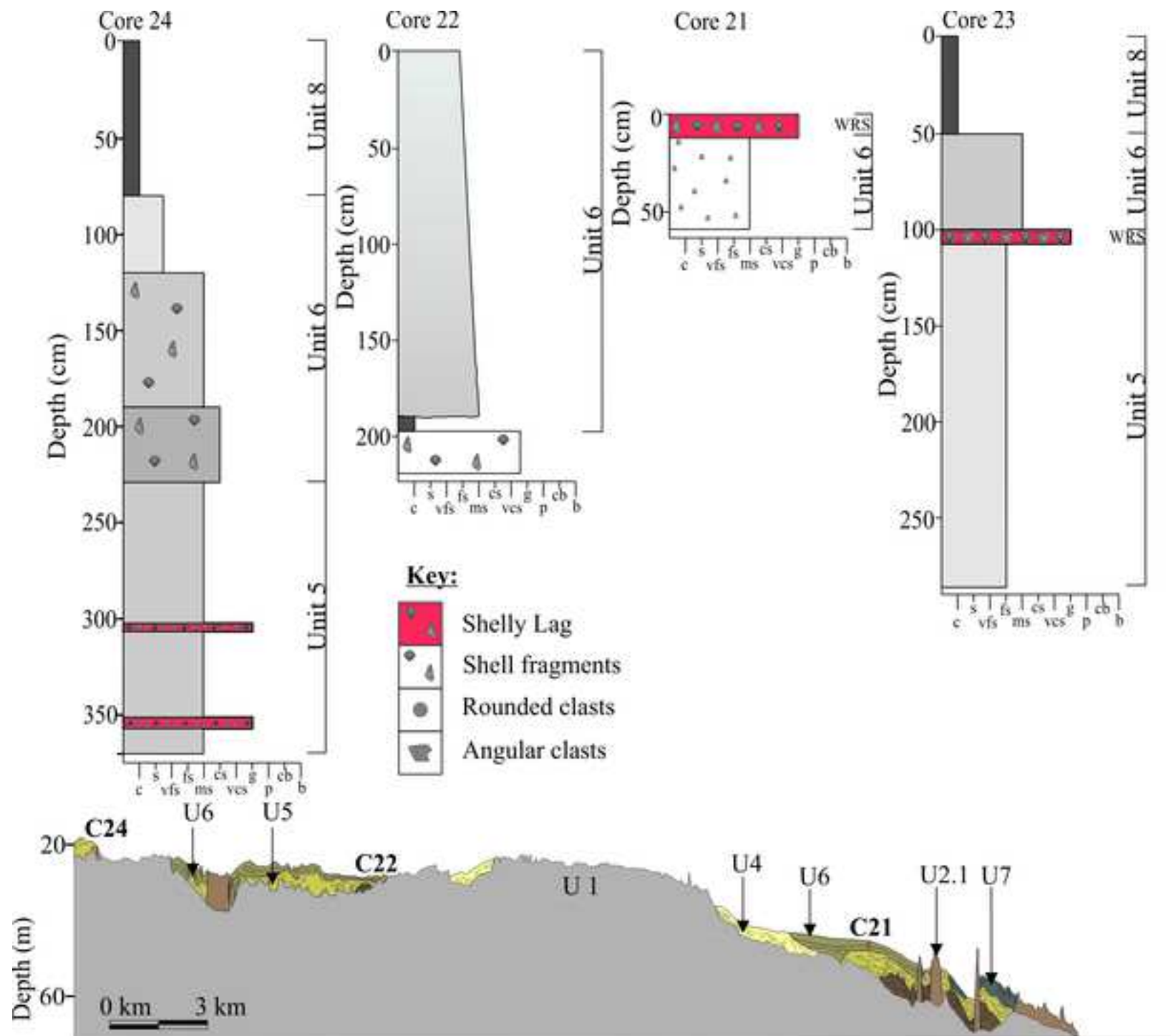


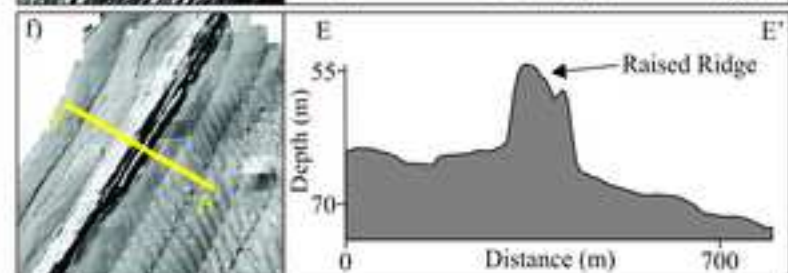
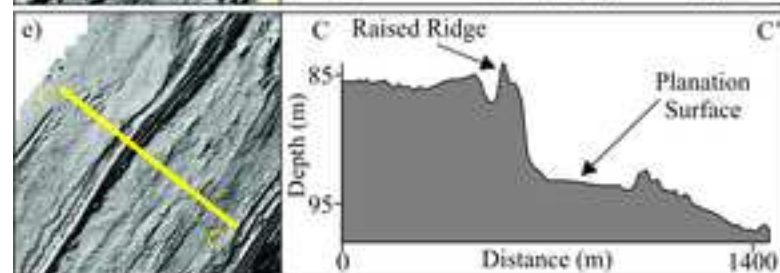
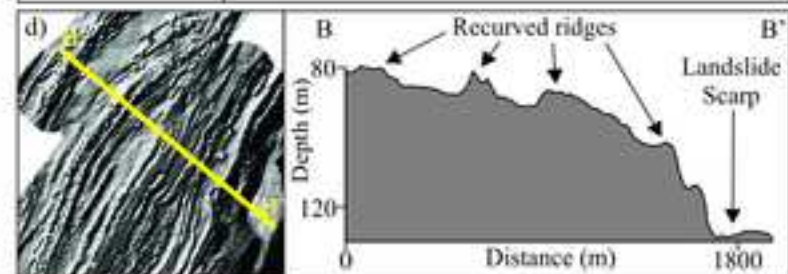
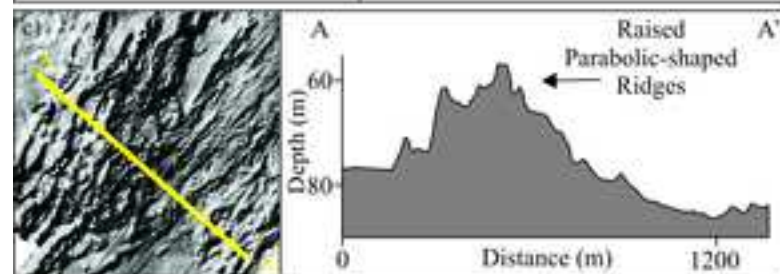
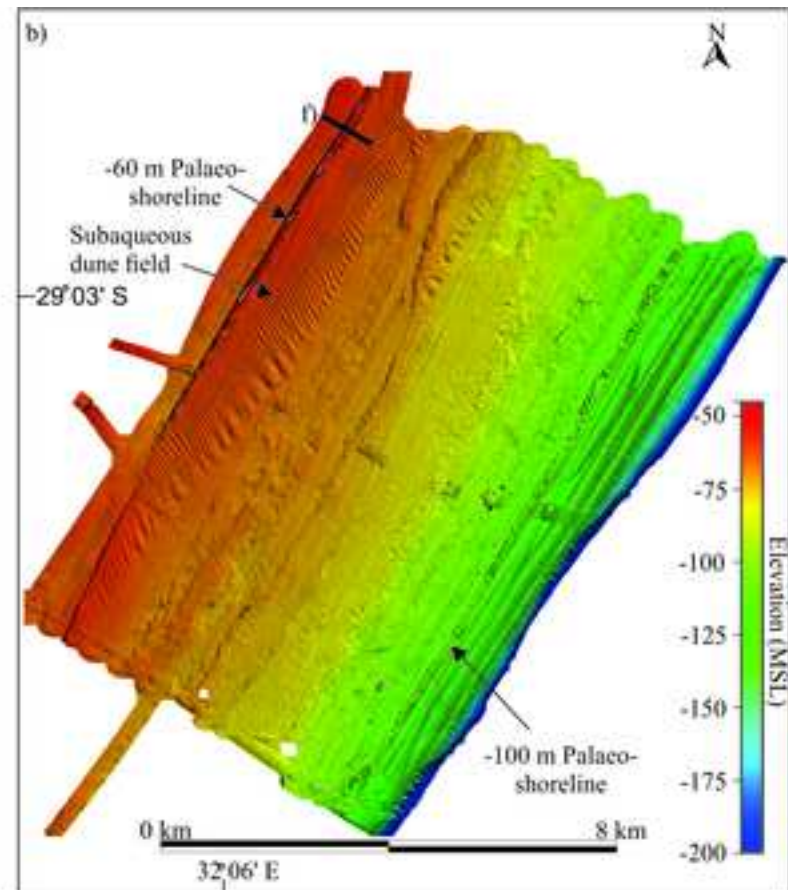
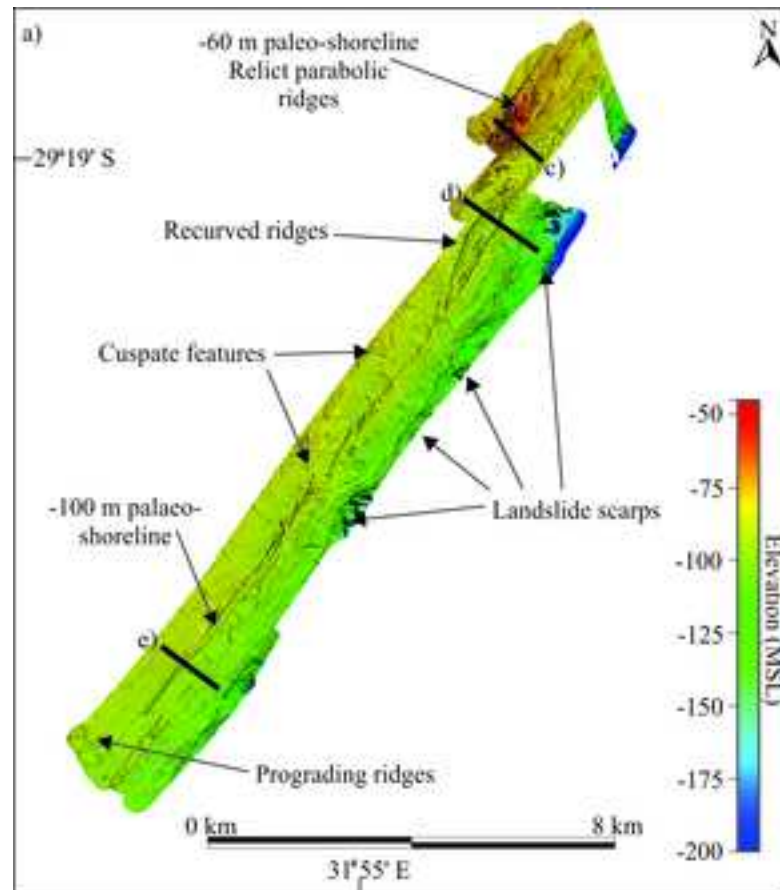


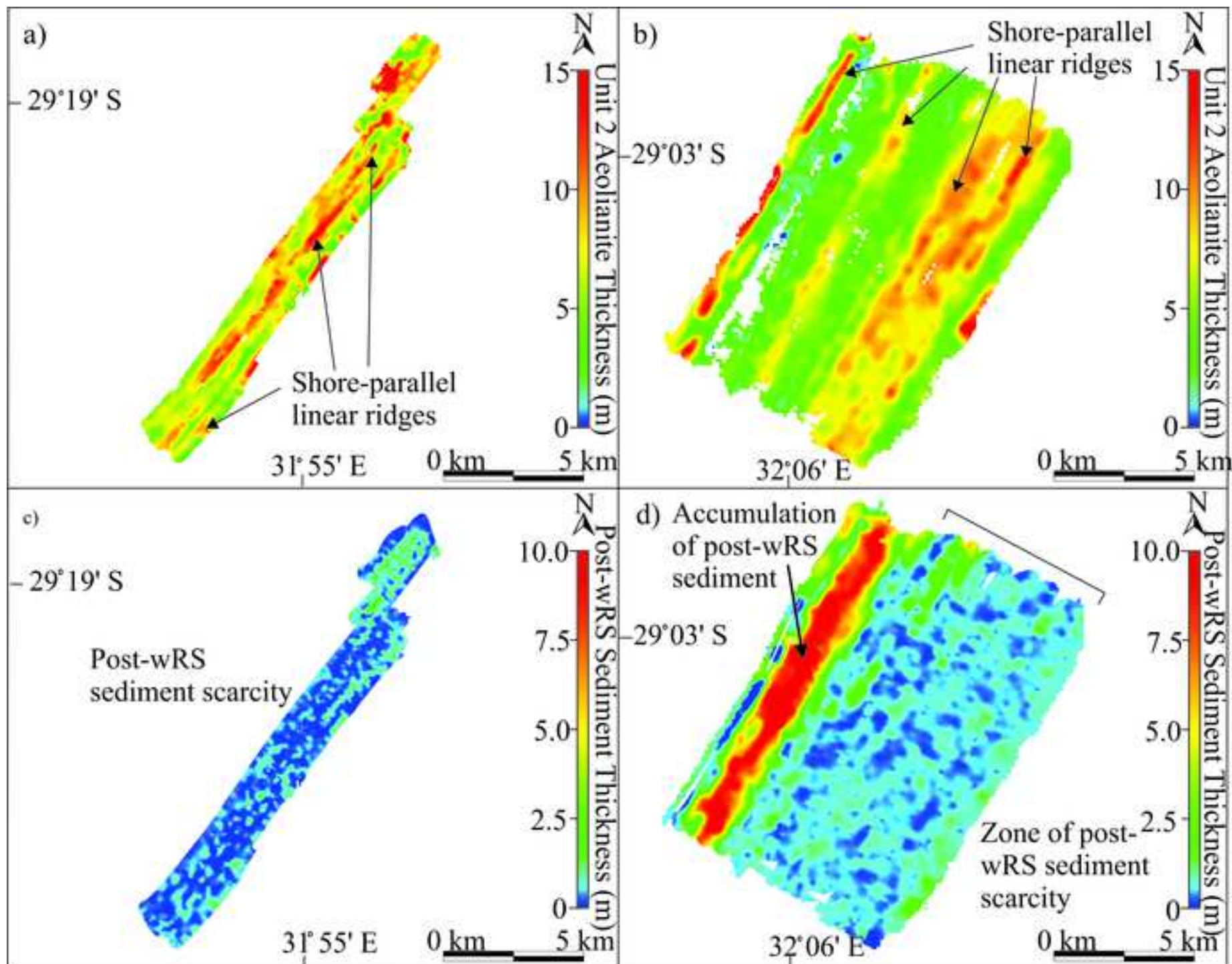


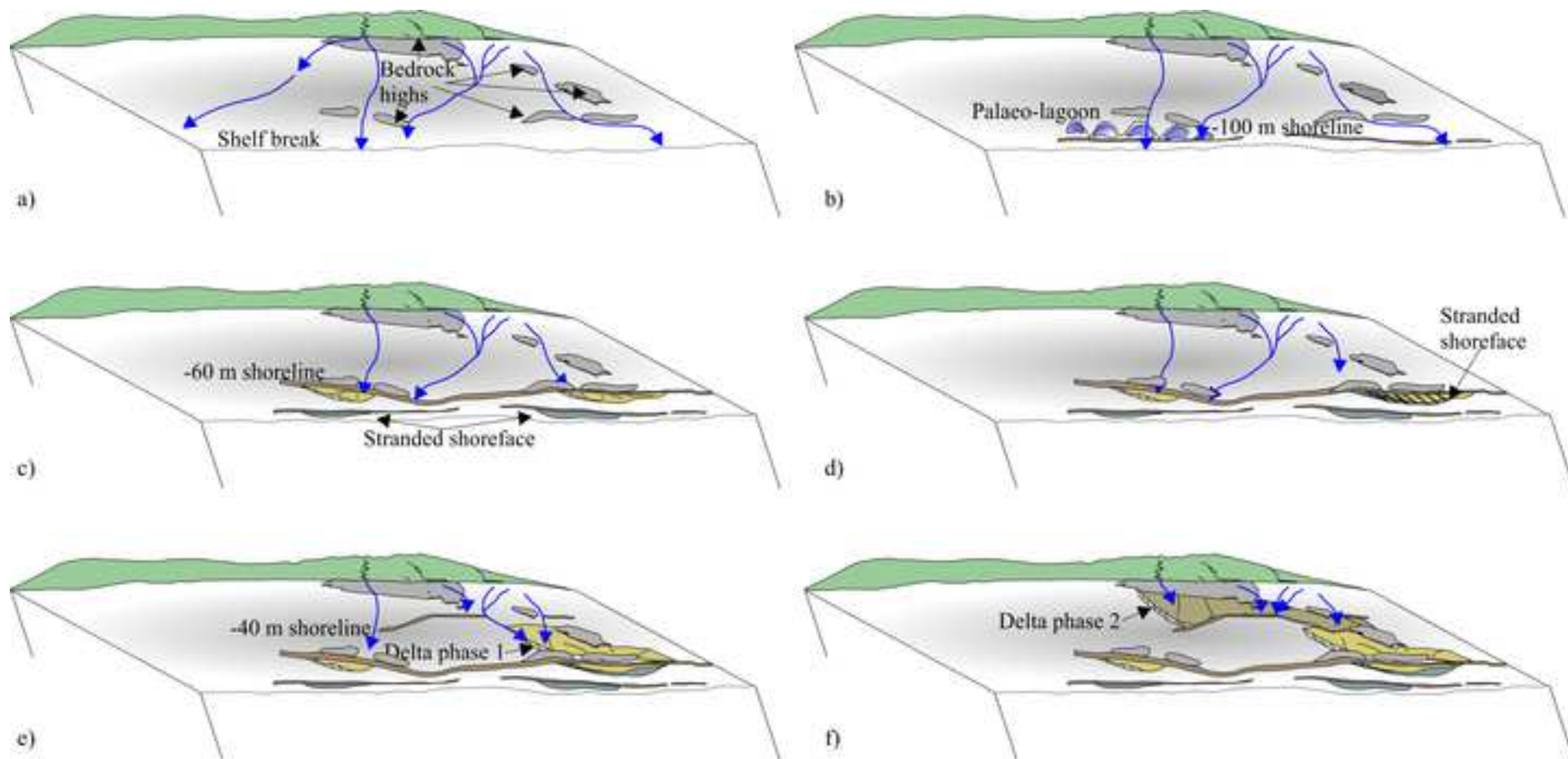


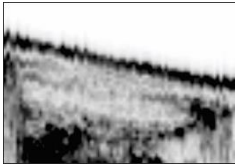
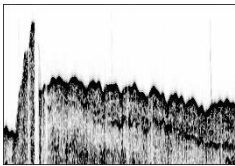
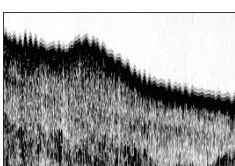
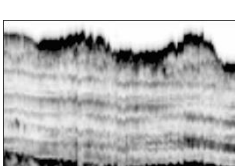
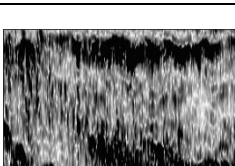
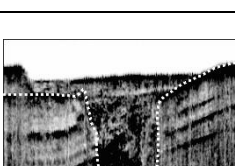
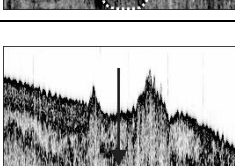
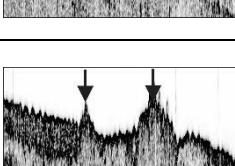










Unit	Underlying surface	Description	Thickness (m)	Seismic-stratigraphic characteristics	Interpretation	Representative unit example
8	Wave ravinement surface	Onlapping sediment draping underlying packages	< 5	Flat lying, continuous, aggradational extremely low amplitude to transparent parallel reflectors	Contemporary prodelta	
7	Wave ravinement surface	Sediment, with undulatory upper surface.	<8	Moderate to high amplitude prograding reflectors.	Detached Shoreface	
6		a) Progradational to mounded facies b) Draped facies	< 8	Low to moderate flat-lying to progradational reflectors	Distal delta front/proximal prodelta	
5		a) Flat lying facies b) Progradational facies	< 15	Low to moderate flat lying to progradational reflectors. Isolated mounds.	Delta top/ proximal delta front	
4	SB1	Flat-lying, uniformly thick veneer of sediment draping the basement unit	3 - 5	Low to moderate amplitude, flat lying to slightly sigmoid-progradational reflectors	Transgressive marine sand sheet	
3	SB1	Isolated, laterally discontinuous fill	10 - 25	Chaotic low to high amplitude reflectors	Incised valley fill	
2.2	SB1	a) Fill within saddles of Unit 2.1 b) Thinning wedge away from Units 2.1 and 2.2	< 5	Moderate to high amplitude horizontal to sub-horizontal reflectors	Calcarene rubble facies	
2.1	SB1	Mid-outer shelf stranded, high relief sediment outcrop	< 25	Acoustically opaque high-relief pinnacles	Beach/barrier system	

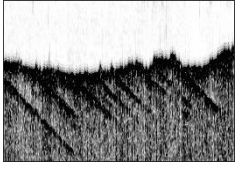
1		Acoustic basement	> 20	High amplitude, continuous seaward-dipping reflectors	Late Pliocene lowstand shelf edge delta	
---	--	-------------------	------	---	---	---

Table 1: Seismic stratigraphy detailing seismic unit descriptions, internal reflector characteristics, unit thickness, interpretation, and representative facies. Arrows mark areas of reference on seismic images.